1854–1870 *Nucleic Acids Research, 2016, Vol. 44, No. 4* *Published online 23 December 2015*
doi: 10.1093/nar/gkv1500

A genome landscape of SRSF3-regulated splicing events and gene expression in human osteosarcoma U2OS cells

Masahiko Ajiro[1,†], Rong Jia[1,†], Yanqin Yang[2], Jun Zhu[2] and Zhi-Ming Zheng[1,*]

[1]Tumor Virus RNA Biology Section, Gene Regulation and Chromosome Biology Laboratory, Center for Cancer Research, National Cancer Institute, National Institutes of Health, Frederick, MD 21702, USA and [2]DNA Sequencing and Genomics Core, System Biology Center, National Heart, Lung, and Blood Institute, National Institutes of Health, Bethesda, MD 20892, USA

Received March 4, 2015; Revised November 29, 2015; Accepted December 11, 2015

ABSTRACT

Alternative RNA splicing is an essential process to yield proteomic diversity in eukaryotic cells, and aberrant splicing is often associated with numerous human diseases and cancers. We recently described serine/arginine-rich splicing factor 3 (SRSF3 or SRp20) being a proto-oncogene. However, the SRSF3-regulated splicing events responsible for its oncogenic activities remain largely unknown. By global profiling of the SRSF3-regulated splicing events in human osteosarcoma U2OS cells, we found that SRSF3 regulates the expression of 60 genes including ERRFI1, ANXA1 and TGFB2, and 182 splicing events in 164 genes, including EP300, PUS3, CLINT1, PKP4, KIF23, CHK1, SMC2, CKLF, MAP4, MBNL1, MELK, DDX5, PABPC1, MAP4K4, Sp1 and SRSF1, which are primarily associated with cell proliferation or cell cycle. Two SRSF3-binding motifs, CCAGC(G)C and A(G)CAGCA, are enriched to the alternative exons. An SRSF3-binding site in the EP300 exon 14 is essential for exon 14 inclusion. We found that the expression of SRSF1 and SRSF3 are mutually dependent and coexpressed in normal and tumor tissues/cells. SRSF3 also significantly regulates the expression of at least 20 miRNAs, including a subset of oncogenic or tumor suppressive miRNAs. These data indicate that SRSF3 affects a global change of gene expression to maintain cell homeostasis.

INTRODUCTION

Alternative pre-mRNA splicing regulates gene expression of ∼92–94% human genes to generate proteomic diversity (1). Aberrant RNA splicing is often associated with various pathological conditions in human, such as myotonic dystrophy (1,2), autism (3), spinal muscular atrophy (4), tauopathies (5) and numerous types of cancer (6). Thus, uncovering of aberrant splicing in any given diseased condition will greatly assist us to understand the genetic determinants of disease (7).

Serine/arginine-rich splicing factor 3 (SRSF3 or SRp20) is the smallest member of serine/arginine-rich (SR) family of proteins and plays important roles in regulation of alternative RNA splicing (8–11), RNA export (12,13) and polyadenylation (14,15), protein translation (16–18), primiRNA processing (19), genome stability (20) and signal pathways (21–24). Altered expression of SRSF3 is found in many human diseases and cancers (25–30). We and others recently reported that SRSF3 has a proto-oncogenic function and is frequently upregulated in various types of cancer (28,31–33). SRSF3 regulates alternative splicing and gene expression of FoxM1 (forkhead box M1), PLK1 (polo-like kinase 1) and CDC25B (cell division cycle 25B) in U2OS osteosarcoma cells (28), and HPV16 (human papillomavirus type 16) E6 and E7 oncogenes in HPV16-positive cervical cancer cells (10). SRSF3 overexpression confers cancerous phenotypes, such as cell cycle progression and antiapoptosis (28,32,34,35), anchorage-independent cell proliferation (28), tumor formation in nude mice (28) and aerobic glycolysis (36), and inhibits replicative senescence (37). Under physiological conditions, SRSF3 regulates the splicing of G6PD (Glucose-6-phosphate dehydrogenase) RNA (38) and hepatocyte differentiation and metabolic function in liver (39). In addition, SRSF3 is one of the major regulators in cell reprogramming of induced pluripotent stem cells (40), implying a possible role in the dedifferentiation process of carcinogenesis. Together, these accumulating evidences strongly suggest a global effect of SRSF3 in the aber-

*To whom correspondence should be addressed. Tel: +1 301 846 7634; Fax: +1 301 846 6846; Email: zhengt@exchange.nih.gov
†These authors contributed equally to the paper as first authors.
Present address: Rong Jia, Key Laboratory of Oral Biomedicine, Chinese Ministry of Education, Wuhan University School of Stomatology, Wuhan, Hubei 430079, China.

rant RNA splicing in cancer cells. Although global analysis of the possible SRSF3-regulated mRNA targets has been performed in mouse neural cell line P19 (41,42), the regulated RNA splicing events and gene expression underlying SRSF3-mediated oncogenesis in human cells remains largely unknown.

In this study, we compared genome-wide profiles of SRSF3-regulated RNA splicing events and gene expression in human osteosarcoma U2OS cells with or without SRSF3 knockdown. We discovered that SRSF3 regulates the expression of at least 224 genes either at the RNA splicing level or at the gene expression level. Most of them are involved in cell cycle or proliferation. SRSF3 also affects the expression of a subset of human miRNAs. This is the first report of a genomic landscape of SRSF3-regulated RNA splicing events and gene expression in human cells.

MATERIALS AND METHODS

Cell cultures and siRNAs

Human osteosarcoma U2OS cells and human cervical cancer HeLa cells were purchased from American Type Culture Collection (ATCC, Manassas, VA, USA). U2OS and HeLa cells were grown in Dulbecco's modified Eagle medium (Invitrogen, Carlsbad, CA, USA) supplemented with 10% fetal bovine serum, 2 mM L-glutamine, 100 U/ml penicillin and 100 μg/ml streptomycin.

SRSF3-specific siRNA (si-SRSF3, cat. No. M-030081–00) and SRSF1 (SF2/ASF)-specific siRNA (si-SRSF1, cat. No. M-018672–01) were purchased as a siGenome SMARTpool siRNA from Dharmacon (Lafayette, CO). A non-targeting siRNA (si-NS) obtained from Dharmacon, with 52% GC content (cat. No. D-001206–08–20), was used as an siRNA control. The SRSF3-specific siRNA s12732, targeting a splice junction of SRSF3 exon 2 and exon 3, was purchased from Ambion (Austin, TX, USA). Cell transfection and siRNA knockdown assays were described in our previous publication (28).

Plasmids and transfection

Minigenes constructed to express EP300 exon 13–15 with or without point mutations in the SRSF3-binding site in mammalian cells were carried out by using pEGFP-N1 (43). Briefly, an EP300 exon 13–15 DNA fragment in size of 2975 bps (Ch22:41545042–41548016) was polymerase chain reaction (PCR)-amplified from HeLa cell genomic DNA, and subcloned into pEGFP-N1 plasmid at XhoI and NotI sites to exclude the EGFP coding sequence. The resulting plasmid was named as pMA-79. The EP300 intron 14 in size of 1634 bps pMA-79 was then shortened to 1011 bps by deletion of a 623-bp XhoI-HindIII fragment between 262 bp downstream of the intron 5′ ss and 751 bp upstream of the intron 3′ ss to yield plasmid pMA-80. Subsequently, deletions [Δ1 (pMA-81), Δ2 (pMA-82), Δ3 (pMA-83 and Δ4 (pMA-84)] and point-mutations [mt-1 (pMA-86) and mt-2 (pMA-87)] were introduced within the exon 14 by overlapping PCR (44). Primer sets used for the minigene vector construction and RT-PCR detection of exogenous EP300 RNA are summarized in Supplementary Table S1. For the plasmid transfection, HeLa cells at 1.0×10^6 in a 6-cm dish were transfected with 4.0 μg of plasmid by LipoD293 (SignaGen Laboratories, Rockville, MD, USA), and total RNA was extracted 24 h after the transfection.

Splice array analysis for human genes

For the human splice array, U2OS cells were transfected with Dharmacon si-SRSF3 or si-NS twice with an interval of 48 h as described (28). Total RNA at 48 h after the second transfection was purified by TRIzol (Invitrogen) and 50 ng of each total RNA from three biological replicates were then reverse-transcribed and applied for a human genome-wide splice-array assay to profile the expression of 20 649 genes and splicing events of 19 066 genes by using a service provider ExonHit Therapeutics, Inc (Gaithersburg, MD, USA) as described previously (45). ExonHit splice array includes probes designed for both known and predicted exons and exon–exon junctions (Supplementary Figure S1). Sample amplification and labeling was performed using the WT-Ovation Pico RNA Amplification System and the FL-Ovation cDNA Biotin Module v2 (NuGen, Inc., San Carlos, CA, USA). Following the scanning by Affymetrix GeneChip Scanner 3000 7G (Affymetrix, Santa Clara, CA, USA), the raw data were processed by background subtraction through robust multichip average method. Quantile normalization was applied on $\log_2$ transformed dataset. Splicing alterations were analyzed by B/E method, by which a ratio of B probe (exon inclusion) and E probe (exon skipping) was measured, while gene expression level was analyzed through probeset intensities of constitutive exons (Supplementary Figure S1) (45). Top candidate genes were selected based on three criteria: (i) ratio changes in splicing or gene expression levels were >2-fold; (ii) acquired signal intensity was more than a cutoff value of 4.3 on $\log_2$ scale; (iii) false discovery rate (FDR) was controlled at 10% for gene expression changes and 20% for splicing alterations.

The unselected gene transcripts from the B/E method were also searched for the SRSF3-dependent splicing events by Analysis of Variance (ANOVA, Supplementary Figure S2) using the linear model: $Y \sim I + L \cdot X + L \times F \times R$, in which, Y: observed probeset intensities with $\log_2$ transformation; I: baseline for Y, including the probe affiliation information and basic splicing ratio information; L: class labels (with 2 levels: si-SRSF3 and si-NS); X: $\log_2$ of the transcription level changes; F: the type of splicing ratio changes to Y (1, −1, 0); R: $\log_2$ of the inclusion ratio changes; For each event we got 6 * 6 equations (6 probes * 6 array), and the parameters of X and R can be estimated with ANOVA. To test the null hypothesis of 'if $X = 0$ or if $R = 0$', empirical Bayesian analysis method (46) was applied to compute the p-values and then FDR method (47) was adopted to generate q-values. Events with q-values of rejecting $R = 0$ null hypothesis <0.2 and splicing ratio changes >2-fold was considered as the significantly regulated splicing events.

Motif-based sequence analysis

Enriched motifs were performed by MEME (Multiple Em for Motif Elicitation) (48,49) for the SRSF3-dependent skipping/inclusion of alternative exons on the top list from

B/E analysis and those events not on the top list, but validated experimentally in this study. The sequence length analyzed in MEME was limited to 600 nts, with 300 nts upstream and 300 nts downstream of a splice site in an alternative exon, for enrichment of the 6-nt motifs that fulfill the statistical threshold of an *E*-value. The enriched motif occurrence rates between exonic and intronic regions were evaluated by Student's t-test.

RNA pulldown assay

RNA pulldown assays were performed as described previously (10,11) with a minor modification. Briefly, 0.8 nmol of 5′-biotin-labeled RNA oligo nucleotides were rotated in the presence of 50 μl of Neutroavidin beads (Thermo Scientific, Waltham, MA, USA) in 1 × TBS (50 mM Tris–HCl [pH 7.4], 150 mM NaCl) for 2 h in 4°C. Beads were then washed with 1 × TBS three times and further rotated with HeLa cell lysate for overnight at 4°C. Beads were then washed with 1 × TBS three times and bound proteins were eluted by mixing with 40 μl of 2 × Laemmli buffer for Western blot analysis. Following RNA oligos with the motif sequence bolded were used in this study: oMA336 (biotin-5′-CAACAAUU**CCAGCC**CCUGUUCCdTdT-3′) for the motif 1 in EP300 exon 14; oMA337 (biotin-5′-CUCAAACU**CCAGGC**UUCAAGUGdTdT-3′) for the motif1 in CKLF exon 3; oMA331 (biotin-5′-CAGCCCCA**GCAGCA**GCCUCGCUdTdT-3′) for the motif 2 in EP300 exon 14; oMA333 (biotin-5′-UUCGGACA**GCAGCA**GUAUGACAdTdT-3′) for the motif 2 in PKP4 exon 7; oMA365 (biotin-5′-UCUGCUGA**CCAGCC**CCAGCAGCTT-3′) for motif c in EP300 exon 14; oMA366 (biotin-5′-UCUGCUGAUCUGUUCCAGCAGCTT-3′) motif c mt-1 in EP300 exon 14; oMA367 (biotin-5′-UGUGCUGAUCUGUUCUAGCAGUTT-3′) for motif c mt-2 in EP300 exon14. Paired RNA oligos oJR9 derived from an HPV16 exonic splicing enhancer (16ESE) and oJR10 derived from an HPV16 ESE mutant (16ESE mt) (10) or oVM41 and oVM42 derived from KSHV K8β RNA (11) were served, respectively, as a positive and negative control for SRSF3 binding in the RNA pulldown assays.

mRNA decay assay

HeLa cells were transfected with Dharmacon si-NS or si-SRSF3 twice with an interval of 48 h. The cells at 48 h after the second transfection were treated with 10 μg/ml of actinomycin D for 0, 1, 2, 4 and 8 h (50,51). Total RNA was extracted at each time point and treated by DNase TURBO (Life Technologies). The DNase-treated total RNA at 1 μg was reverse-transcribed and quantified by TaqMan real-time PCR for the remaining RNA levels of SRSF3 and GAPDH (Applied Biosystems, Life Technologies). Relative SRSF3 RNA expression levels at individual time points were determined by $\Delta\Delta C_T$ method (52). After normalizing to GAPDH RNA, the SRSF3 RNA decay rates were calculated by setting the RNA levels at 0 h as 100% for both si-NS and si-SRSF1 groups. Exponential fitting curves were determined by the logarithmic least squares method (50).

WST-8 cell proliferation assay

For the WST-8 cell proliferation assay, dehydrogenase activities in living cells were measured by Cell Counting Kit-8 from Dojindo Molecular Technologies (Rockville, MD, USA) as previously described (53–55). Briefly, cells were incubated with 10% WST-8 in culture medium for 40 min at 37°C, and the cell culture medium was then measured in three biological repeats for 450-nm absorbance to calculate the relative cell viability.

RT-PCR

U2OS or HeLa cells were transfected by si-SRSF3, si-NS or si-SRSF1 twice with an interval of 48 h. Total RNA at 48 h after the second transfection was purified by TriPure (Roche Diagnostics) and used for RT-PCR analysis. Following DNase I treatment, total RNA at 1–4 μg was reverse transcribed at 42°C using random hexamers followed by PCR amplification using a pair of gene-specific primers and agarose gel running. The signal intensity of each RT-PCR product in the gel was measured and the background subtraction were performed by Image Lab 3.0 (Bio-Rad Laboratories, Hercules, CA, USA) to determine fold-change or percent splice-in (PSI) as described (56) for each RT-PCR result after normalizing to GAPDH RNA loading control. Gene-specific primers used in the RT-PCR analysis are in the summarized Supplementary Table S1.

Western blot and immunohistochemistry staining

Protein samples collected along with total RNA at the same time in U2OS and HeLa cells or from the RNA oligo pulldown assays in 2× Laemmli buffer were denatured by boiling for 5 min, separated by sodium dodecyl sulphate-polyacrylamide gel electrophoresis, transferred to a nitrocellulose membrane, and blotted with the following antibodies: mouse monoclonal anti-SRSF3 (7B4, ATCC), anti-β-tubulin (BD PharMingen, San Diego, CA, USA), anti-β-actin (AC-15, Santa Cruz Biotechnology, Santa Cruz, CA, USA), anti-hnRNP K (D-6, Santa Cruz Biotechnology), anti-p300 (Abcam, Cambridge, MA, USA), anti-CHK1 (G-4, Santa Cruz Biotechnology), anti-SRSF1 (clone 96, Invitrogen) and anti-PTB (SH54, Santa Cruz Biotechnology), and rabbit polyclonal anti-Annexin A1 (Abcam), anti-ERRFI1 (ProteinTech, Chicago, IL, USA) and anti-TGFβ2 (Santa Cruz Biotechnology) antibodies. Phopsphorylated pan-SR proteins were detected with mAb104 (ATCC). Quantification of signal intensities and background subtractions in Western blot were performed by Image J (57).

Immunohistochemical staining of cervical tissue sections purchased from US BioMax (Rockville, MD, USA) was performed as described (28) by following antibodies: mouse monoclonal anti-Annexin A1 (clone 29, BD Biosciences, San Jose, CA, USA), anti-involucrin (SY5, Santa Cruz Biotechnology), anti-hnRNP A1 (4B10, Santa Cruz Biotechnology), anti-hnRNP K (D-6, Santa Cruz Biotechnology), anti-hnRNP L (4D11, Abcam), anti-SRSF1 (clone 96, Invitrogen,), and anti-SRSF2 (Sigma-Aldrich, St Louis, MO, USA) and rabbit polyclonal anti-YB1 antibody (Abcam).

Pathway enrichment analysis

Conditional hypergeometric test in the GOstats package (58) at http://www.bioconductor.org/packages/release/bioc/html/GOstats.html was adopted to find out the regulated splicing events significantly enriched biological pathways with a *P*-value <0.01.

Micro-Paraflo miRNA microarray assay, Northern blot and TaqMan miRNA real-time quantitative RT-PCR assays

Human microRNA array assay was performed using a service provider (LC Sciences, Houston, TX, USA). Total RNA isolated from HeLa cells with or without SRSF3 knockdown (three repeats for each) was analyzed for a genome-wide expression of 856 human mature miRNAs. A subset of miRNAs with a significant change in their expression were randomly selected for further confirmation by Northern blot or by TaqMan miRNA real-time quantitative RT-PCR assays as described (59–61). U6 snRNA served as an internal loading control. All of the TaqMan microRNA and U6 snRNA probes were purchased from Applied Biosystems of Life Technologies.

RESULTS

Global identification of SRSF3-regulated splicing events and gene expression in human U2OS cells

To understand SRSF3-induced changes in RNA splicing and gene expression, we performed ExonHit SpliceArray analysis (45) to profile the expression of 20 649 genes and the 138 636 splicing events of 19 066 genes for human U2OS cells with or without SRSF3 knockdown. Based on three criteria stated in 'Materials and Methods' section: (i) a threshold of ≥2-fold change in $\log_2$ as determined by a B/E method for an alternative splicing event or by probeset intensities of constitutive exons for a gene expression level, (ii) FDR value <0.1 for gene expression changes and <0.2 for splicing alterations, and (iii) acquired signal intensity >4.3 on $\log_2$ scale, we identified a large set of SRSF3 targets with highly responsive events (Figure 1 and Supplementary Table S2, see NCBI GEO accession no. GSE22149 for the full list). These identified targets with altered events are categorized into three groups: evidenced splicing events in which the identified splicing variants have been previously reported; novel splicing events in which the identified splicing variants have not been reported, or predicted only *in silico*; gene expression change in which gene expression levels are increased or decreased following SRSF3 knockdown. The top SRSF3-responsive events consist of 43 evidenced splicing events from 40 genes, 14 novel splicing events from 14 genes (Figure 1A and B and Supplementary Table S2) and 62 genes with changes of the expression level (Figure 1C and Supplementary Table S3). However, knocking down SRSF3 in U2OS cells was found to alter the expression of ERRFI1 and DDEF2 both at RNA splicing and at gene expression level (Figure 1).

SRSF3-regulated genes are primarily associated with regulation of cell proliferation and RNA splicing and their primary transcripts contain highly conserved RNA motifs

Classification of those SRSF3-regulated genes by pathway enrichment revealed that SRSF3 primarily targets the expression of those genes associated with cell growth, cell cycles, cell cytoskeleton and RNA splicing (Figure 2A), which are in concordance with the described roles of SRSF3 in cell proliferation (28,32,34). We further looked into the enriched motifs for the SRSF3-responsive splicing events by MEME analysis (48,49). Subsequently, we identified two consensus A/C-rich motifs, motif 1 CCAG(C/G)C and motif 2 (A/G)CAGCA. These two motifs were especially enriched in the exonic region ∼50–150 nts from the splice sites in the alternative exons (Figure 2B and C, Supplementary Table S4), but much less in the intron region (Figure 2B and C), with the motif 2 being a typical case (Figure 2C). Both motifs were common upstream of the 5′ splice sites (5′ ss, Figure 2C), but the motif 1, not the motif 2, was the only motif enriched in the exon region downstream of the 3′ splice sites (3′ ss, Figure 2B). The motif 1 was enriched relatively more often than the motif 2 in the intron regions either upstream of 3′ ss or downstream of the 5′ ss of the alternative exons (Figure 2B and C). Two enriched motifs are similar to the previously reported SRSF3 binding site (C/U)(A/C/U)(U/A)(C/A/U)(A/C/U) identified by a CLIP (cross-linking immunoprecipitation) assay in mouse neural P19 cells (42). A/C-rich elements was previously identified in CD44 (62), bovine papillomavirus 1 (BPV1) (44) and HPV16 transcripts (10), and characterized as an SRSF3-binding site in regulation of alternative RNA splicing (10). Accordingly, we performed SRSF3 RNA-binding assays for the RNA motif 1 and motif 2 identified in EP300 exon 14, CKLF exon 3 and PKP4 exon 7, with SRSF3-binding HPV16 ESE wt and mt, respectively, as a positive and negative control (10). Using HeLa cell extract and a synthetic RNA oligo containing the motif 1 or motif 2 for RNA pull-down assay, we found that both motif 1 and motif 2 in its native context bind SRSF3 (Figure 2D).

SRSF3 regulates gene expression of ERRFI1, ANXA1, and TGFB2 and alternative RNA splicing of PUS3, PKP4, KIF23, EP300 and CLINT1

We subsequently validated by RT-PCR a subset of the identified alterations of gene expression and splicing events both in U2OS and HeLa cells. These include SRSF3-regulated expression changes (≥50%) of ERRFI1, ANXA1 and TGFB2 (Figure 3A–C) in either cell type. We confirmed SRSF3 knockdown increases the expression of ERRFI1 (Figure 3A) and ANXA1 (Figure 3B), but decreases the expression of TGFB2 (Figure 3C), at the RNA level.

The criteria for validation was based on (i) detection of an aberrant splicing product(s) from agarose gel electrophoresis, (ii) the aberrant splicing product(s) has a PSI ≥10% from either cell type and (iii) the aberrant splicing event is repeatedly detectable by another si-SRSF3 approach. Validation of the SRSF3-regulated alternative RNA splicing events were carried out for PUS3, PKP4, KIF23, EP300 and CLINT1 (Figure 3D–H). We confirmed that SRSF3 knockdown induces the selection of an alternative 5′ ss in

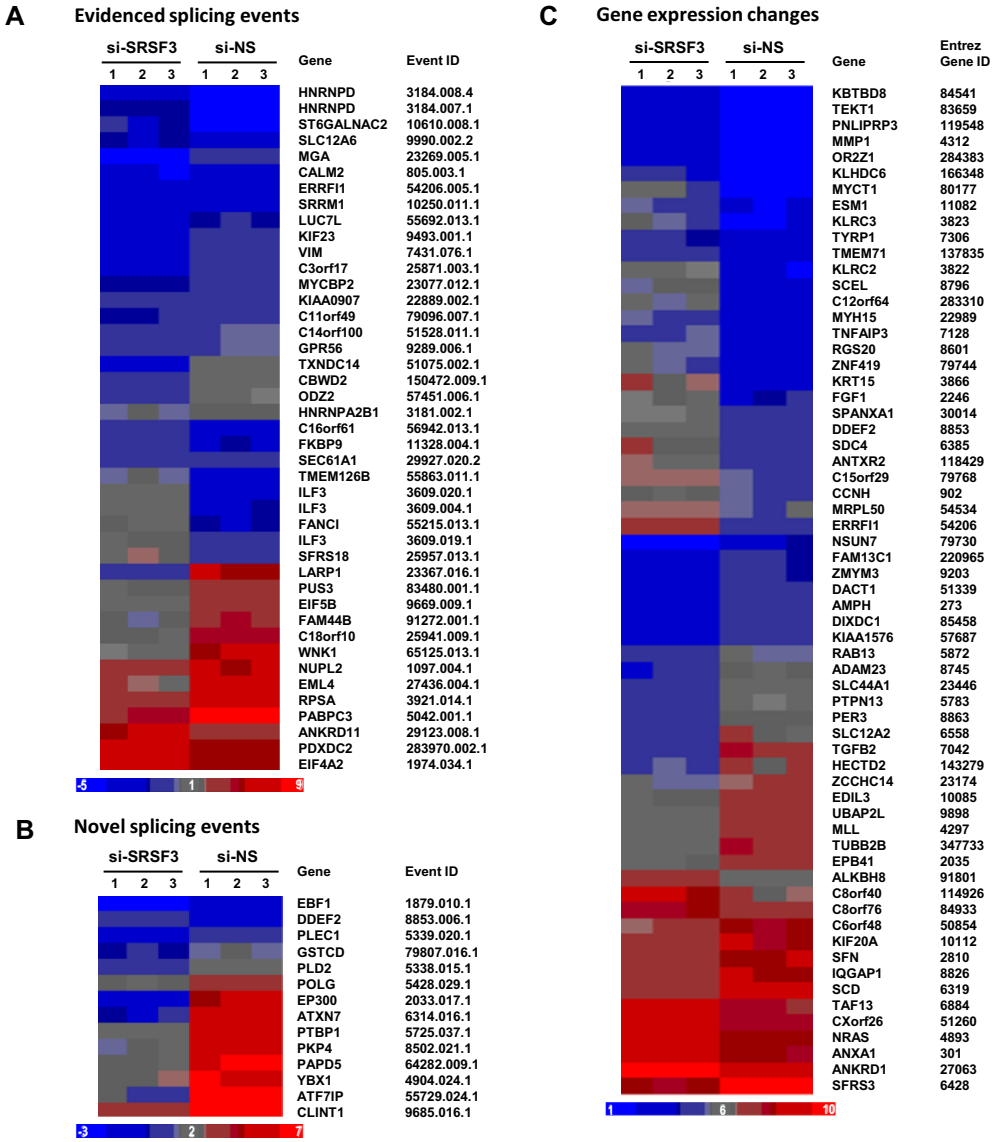

Figure 1. SRSF3-targeted splicing events and changes of gene expression in U2OS cells. (**A**–**C**) Clustered heat maps for the top events regulated by SRSF3 identified by ExonHit splice arrays. SRSF3-targeted genes in three experimental repeats consist of 43 evidenced splicing events from 40 genes (A), 14 novel splicing events from 14 genes (B) and 62 gene with expression changes (**C**), with a threshold of ≥2-fold changes in $\log_2$ as determined by a B/E method and FDR cutoff of 0.1 for gene expression change and 0.2 for splicing alternation. Individual gene names and event ID are indicated on the right. Event ID specifies individual splicing events being detailed in Supplementary Table S2. SRSF3 expression level in U2OS cells with si-SRSF3 or si-NS treatment was included in (C) as a control. Color key scales in $\log_2$ values are indicated at the bottom of each panel. The full list of B/E ratio analysis result is available at NCBI GEO (http://www.ncbi.nlm.nih.gov/geo/) (accession number GSE22149).

the PUS3 exon 3 (Figure 3D) and promotes exon skipping of PKP4 exon 7 (Figure 3E), KIF23 exon 18 (Figure 3F), EP300 exon 14 (Figure 3G) and CLINT1 exon 11 (Figure 3H). In addition, we found both Dharmacon and Ambion siRNAs targeting to different regions of SRSF3 displayed the similar results for KIF23, EP300 and CLINT1 (Figure 3F–H). We also validated three splicing events of ILF3 regulated by SRSF3, but failed to confirm the SRSF3-regulated PLD2 splicing event. Together, the B/E ratio analysis provides a confirmation rate of ∼91% by RT-PCR for the SRSF3-regulated gene expression and RNA splicing events (Supplementary Table S5).

SRSF3 regulates alternative RNA splicing of CHK1, SMC2, CKLF, MAP4K4, MBNL1, MELK, DDX5, PABPC1, MAP4K4, Sp1 and SRSF1

We further analyzed by ANOVA (analysis of variance) on those events under the threshold in the B/E ratio calculation. ANOVA examines the intensities of all six probes as diagrammed in Supplementary Figure S1 to improve statistical power for detection of splicing change. As a result, we identified additional 122 splicing events in 114 genes (Supplementary Figures S2 and S3, Table S6) with significant changes (>2-fold), including seven gene transcripts identified by the B/E method. We further selectively validated the SRSF3-regulated exon skipping of the CHK1 exon 3,

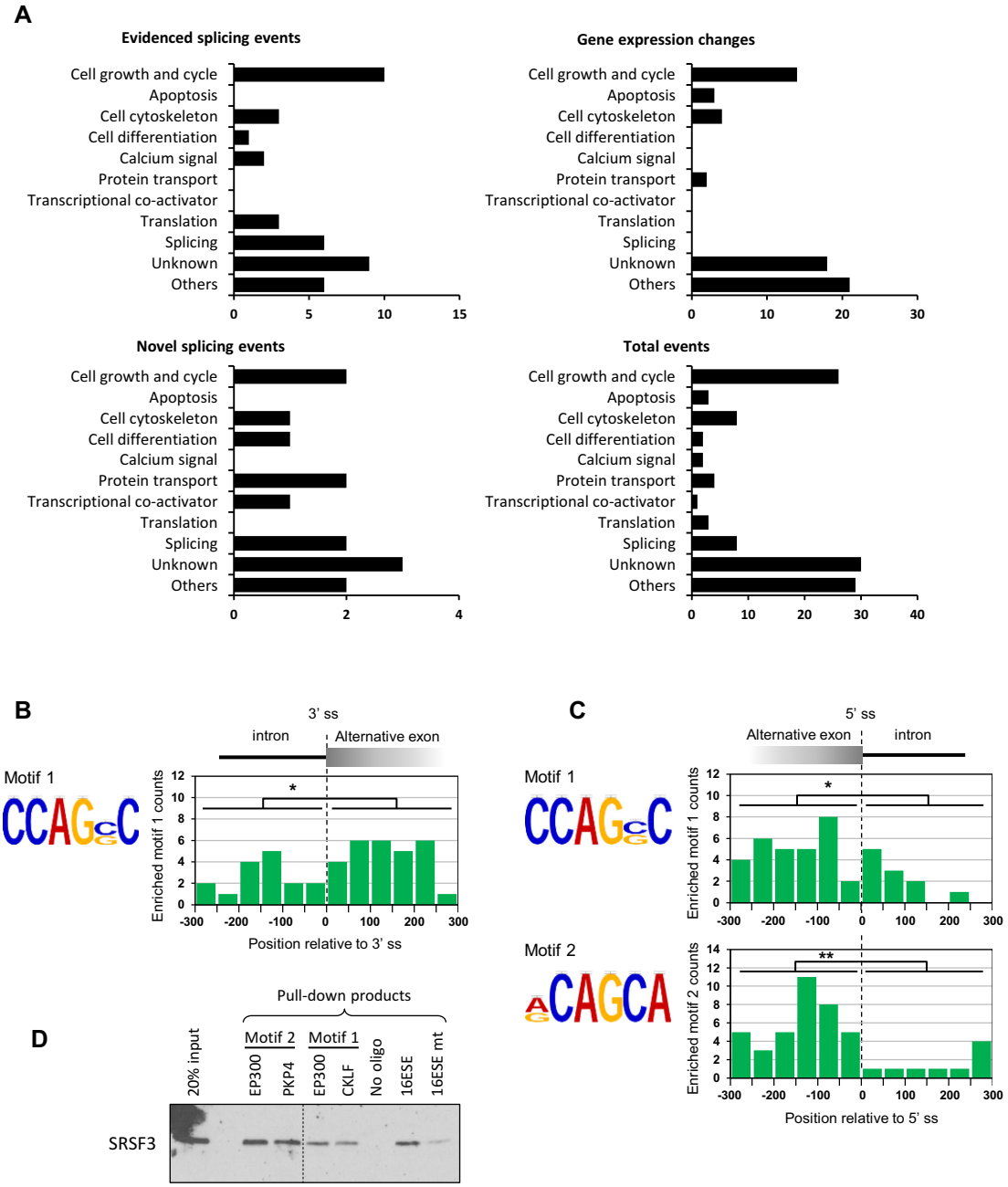

Figure 2. Functional classification and MEME motif analysis of the identified SRSF3-responsive targets. (**A**) Functional classification of the SRSF3-responsive targets with alternative splicing (evidenced and novel splicing) events and gene expression changes. (**B** and **C**) Identification of enriched motifs in SRSF3-responsive alternative exons. Three hundred nucleotides (nts) upstream and downstream of 3′ splice site (3′ ss, B) or 5′ splice site (5′ ss, C) of SRSF3-responsive alternative exons were search for enriched motifs by MEME. MEME motifs are represented by sequence LOGO derived from position-specific probability matrices. A single motif around the 3′ ss (B) and two motifs around the 5′ ss (C) were identified. Each motif occurrence was counted by 50 nts as window size up to 300 nts upstream or downstream of 3′ ss or 5′ ss of alternative exons. $*P < 0.05$; $**P < 0.01$ by Student's *t*-test. (**D**) SRSF3 in HeLa cell extract binds to the enriched motif 1 and motif 2 from EP300 exon 14, CKLF exon 3 and PKP4 exon 7 by RNA pull-down assays. HPV16 ESE (16ESE) or its mutant (16ESE mt) RNA oligo (10) served as a positive or negative control. One representative experiment of two is shown.

SMC2 exons 3–4, CKLF exon 3, MAP4 exon 10, MBNL1 exon 4, MELK exon 11, DDX5 exon 12 and PABPC1 exons 10–11. As shown in Figure 4, knocking down SRSF3 expression in U2OS and HeLa cells induces exon skipping of these gene transcripts (Figure 4A–H). Both siRNAs targeting to SRSF3 from Dharmacon and Ambion exhibited a similar result (Figure 4C–H). However, we failed to validate NUMB and NASP for their altered splicing events identified by ANOVA analysis. Together, ANOVA analysis provides a confirmation rate of ∼82% by RT-PCR for the SRSF3-regulated splicing events (Supplementary Table S5).

We also selectively examined three additional gene transcripts with SRSF3-altered splicing change not on the ANOVA top list, but close to the threshold value, either in

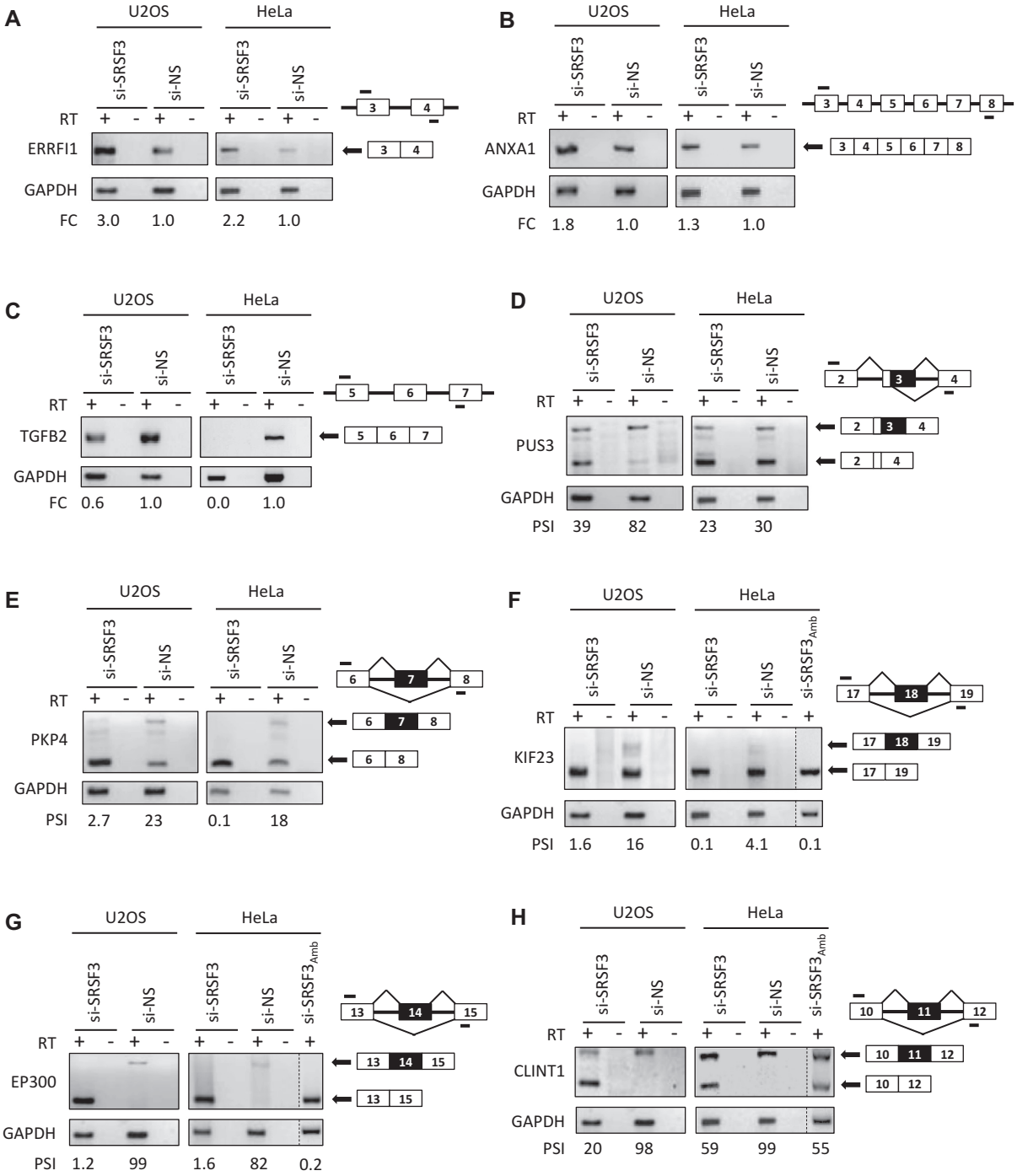

Figure 3. Validation of the SRSF3-responsive events identified by B/E ratio analysis. U2OS and HeLa cells were transfected with Dharmacon si-NS or si-SRSF3 twice in an interval of 48 h. Total RNA from the cells were analyzed by RT-PCR to validate transcript level change of ERRFI1 (**A**), ANXA1 (**B**) and TGFB2 (**C**), splicing alteration of PUS3 alternative 5′ ss usage in the exon 3 (**D**), and exon skipping of the PKP4 exon 7 (**E**), KIF23 exon 18 (**F**), EP300 exon 14 (**G**) and CLINT1 exon 11 (**H**). The primers used in RT-PCR are shown as bars above (forward primers) and below (reverse primers) each RNA splicing diagram. GAPDH served as a loading control. RT+, reaction with reverse transcriptase; RT−, reaction without reverse transcriptase; si-SRSF3$_{Amb}$, si-SRSF3 from Ambion; FC, fold-change; PSI, percent spliced-in of the alternative exon(s) or splice site (% inclusion = inclusion/sum of inclusion + exclusion).

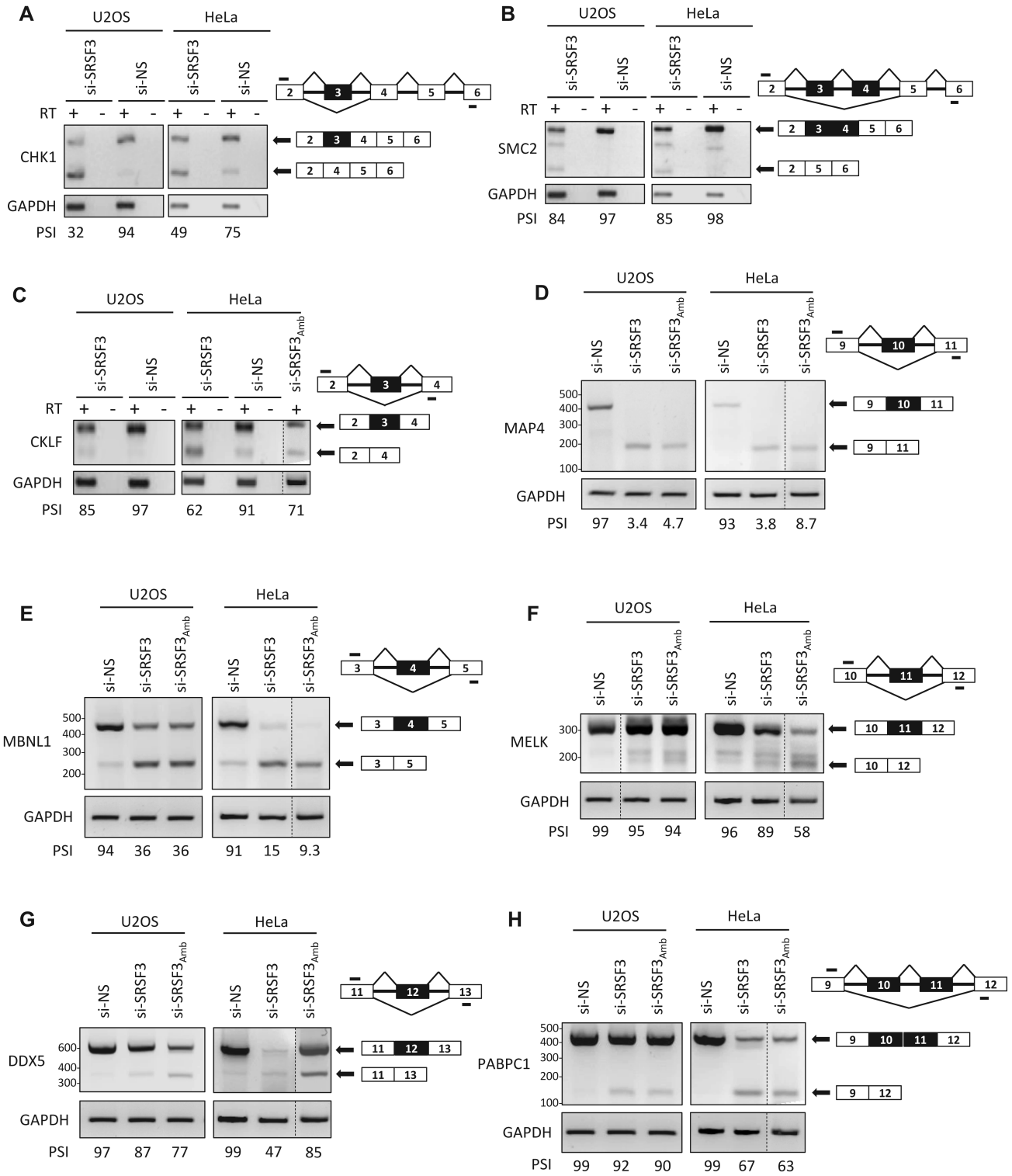

Figure 4. Validation of other SRSF3-responsive RNA splicing events identified by ANOVA analysis. Following transfection of U2OS or HeLa cells with Dharmacon si-NS or si-SRSF3 twice in an interval of 48 h, total RNA from the cells was analyzed by RT-PCR for exon skipping of CHK1 exon 3 (**A**), SMC2 exon 3–4 (**B**), CKLF exon 3 (**C**), MAP4 exon 10 (**D**), MBNL1 exon 4 (**E**), MELK exon 11 (**F**), DDX5 exon 12 (**G**) and PABPC1 exon 10–11 (**H**). See other details in Figure 3.

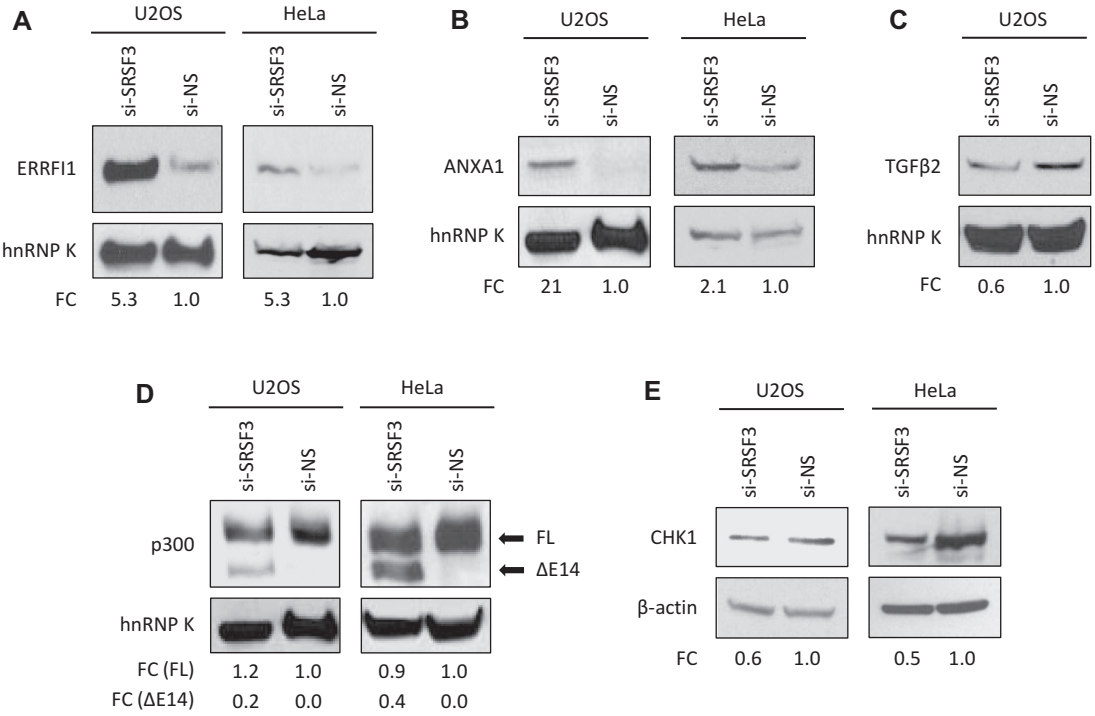

Figure 5. Validation for protein expression changes following SRSF3 knockdown in U2OS and HeLa cells. U2OS and HeLa cells were transfected with Dharmacon si-NS or si-SRSF3 twice with an interval of 48 h. Whole cell lysates at 48 h after the second transfection were analyzed by Western blotting for ERRFI1 (**A**), ANXA1 (**B**), TGFβ2 (**C**), p300 (**D**) and CHK1 (**E**). hnRNP K or β-actin served as a sample loading control. FL, full length p300; ΔE14, p300 isoform produced by exon 14 skipping; FC, fold-change.

U2OS or HeLa cells or both. Knocking down SRSF3 expression induces skipping of the MAP4K4 exon 23alt (Supplementary Figure S4A) and selection of an alternative 3′ ss in the Sp1 exon 3 (Supplementary Figure S4B), but activates a cryptic intron within the exon 4 of SRSF1 (ASF/SF2) in HeLa cells (Figure 7A). Data suggest that many other splicing events not on the ANOVA top list (Supplementary Table S6), but in our submitted datasets (see NCBI GEO accession no. GSE22149 for the full list) might be still true SRSF3 targets.

SRSF3-regulated transcription and RNA splicing events alter protein production of the regulated genes

We further selected randomly five SRSR3-targeted genes identified by B/E and ANOVA analyses and confirmed their changes at RNA transcription or splicing level for their possible changes at protein level in U2OS and HeLa cells. As expected, knocking down SRSF3 in these cell lines increases the expression of ERRFI1 and ANXA1 proteins (Figure 5A and B), but decreases the expression of TGFβ2 protein (Figure 5C). In addition, SRSF3 knockdown induces skipping of the EP300 exon 14 (Figure 3G) to cause in-frame deletion of the p300 bromodomain and consequently the production of a shorter isoform p300 protein which we named p300ΔE14 (Figure 5D). We also confirmed that SRSF3 knockdown decreases the expression of full-length CHK1 protein (Figure 5E) by induction of skipping of the CHK1 exon 3 to create a premature stop codon after the first 29 amino acid residues (Figure 4A).

An SRSF3-binding site is required for inclusion of the EP300 exon 14

We next explored the SRSF3 binding in functional correlation with its regulation of EP300 exon 14 skipping. EP300 was chosen because its encoded p300 protein, a well-known histone acetyltransferase, promotes transcription through histone acetylation (63–65). A minigene expressing EP300 exon 13–15 was first subcloned into a pEGFP-N1 vector under the control of a CMV IE promoter, with a truncation in the middle of the intron 14. Subsequently, four putative SRSF3-binding motifs (a, b, c and d) identified by MEME in the exon 14 were separately deleted in the order in each designated subclone Δ1, Δ2, Δ3 and Δ4 (Figure 6A) and examined in HeLa cells by transient transfection for skipping of the EP300 exon 14. We found that deletion of the SRSF3-binding motif c, but not the binding motifs a, b or d, significantly promotes the skipping (Figure 6B and C), indicating that the SRSF3-binding motif c is responsible for inclusion of the exon 14. To further confirm this observation, we introduced point mutations into the motif c, which has a motif 1 sequence (Figure 2B and C), and its surrounding sequence (Figure 6D), and examined for its binding by SRSF3. As expected, the motif c RNA, but not its mt-1 and mt-2 RNAs, binds SRSF3 (Figure 6E). Both mt-1 and mt-2 RNAs, but not the wt motif c, bind PTB and in addition, the mt-2 RNA binds ∼30-kDa SR protein recognizable by mAb104 (Figure 6E), but not by anti-SRSF1 (data not shown). The loss of SRSF3, but PTB binding to the mt motif c, significantly increases skipping of the exon 14 (Figure 6F and G). The mt-2 minigene containing ad-

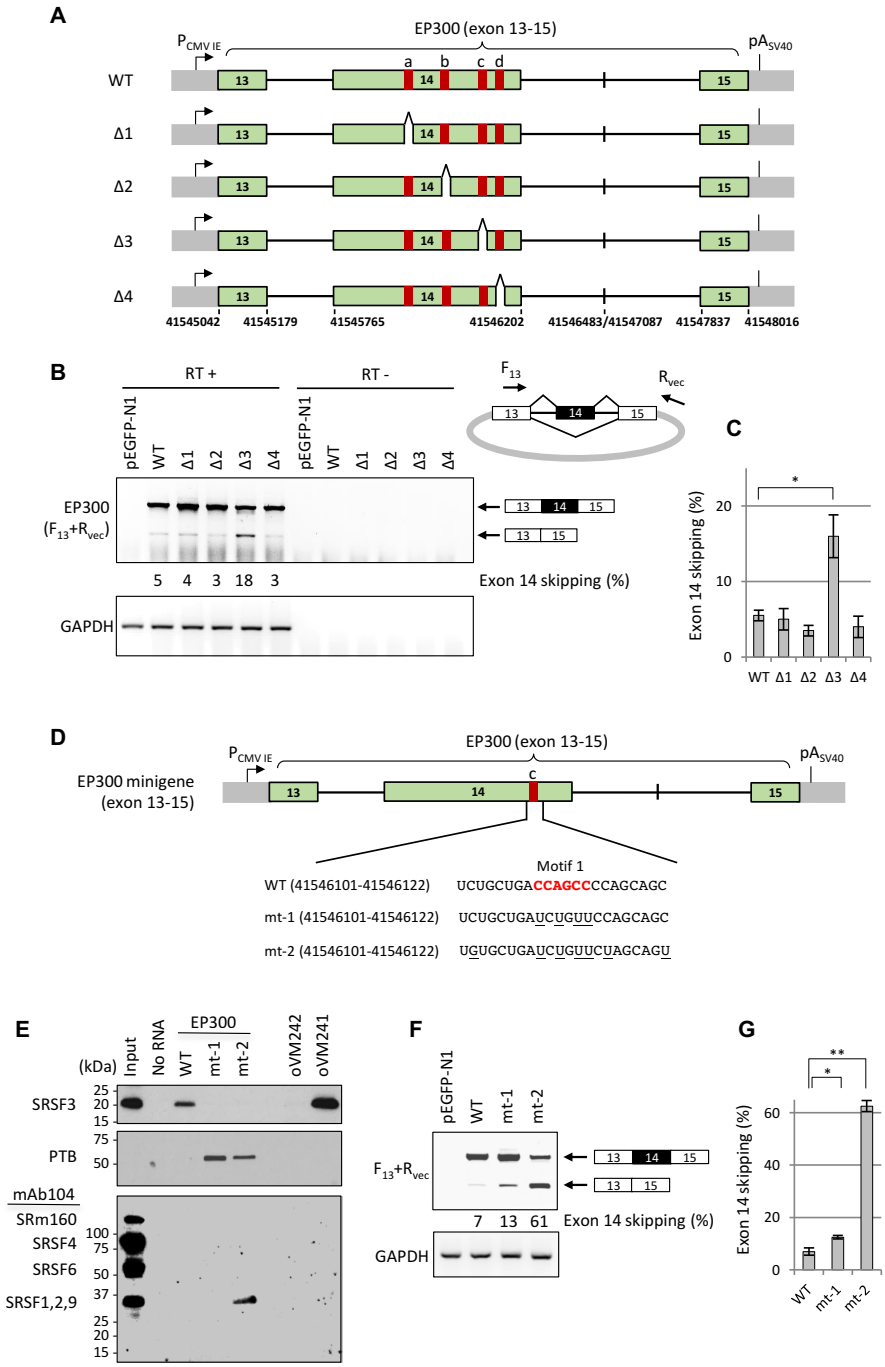

Figure 6. SRSF3 promotes inclusion of the EP300 exon 14 through an exonic SRSF3-binding site. (**A**) Diagram of EP300 minigene structure and exon 14 mutants containing detection (Δ1, Δ2, Δ3 and Δ4) of a 6-nt, putative SRSF3-binding motif. Red boxes a, b, c and d indicate individual putative SRSF3-binding motif. The EP300 minigene has a 623-bp deletion in the intron 14 indicated by a vertical line. $P_{CMV\ IE}$, cytomegalovirus immediate early promoter; pA_{SV40}, SV40 polyadenylation signal. (**B** and **C**) Deletion of a putative SRSF3-binding motif increases skipping of the EP300 exon 14. HeLa cells were transfected with individual EP300 minigenes or a parental vector pEGFP-N1 for 24 h, and skipping of the minigene exon 14 was determined by RT-PCR with a primer set for EP300 exon 13 (F_{13}, forward primer) and vector sequence (R_{vec}, reverse primer, diagrammed on the right). GAPDH RNA served as a loading control. RT-PCR products were resolved by gel electrophoresis, the band intensity was measured, and after normalizing to GAPDH RNA, a skipping rate (%) of the EP300 exon 14 was calculated. Shown in bar graphs (C) are means ± SD from two separate experiments. $^{*}P < 0.05$ by Student's *t*-test. (**D**–**G**) Introduction of point mutations into the SRSF3-binding motif c in the EP300 exon 14 disrupts its SRSF3 binding and splicing activity. Schematic diagram of the SRSF3-binding motif c in the exon 14 of the EP300 minigene construct is shown in (D), with its sequence motif (red) for wt and mt-1 or -2 containing point mutations (nucleotides underlined). Synthetic RNA oligos with the indicated RNA sequence in (D) were examined for binding of SRSF3, PTB and other SR proteins using HeLa nuclear extract and Western blot assays with indicated antibodies (E). Kaposi's sarcoma associated herpesvirus K8β RNA oligos oVM241 and oVM242 in (E) are positive and negative SRSF3 binding controls (11). HeLa cells transfected with individual EP300 minigenes or a parental vector pEGFP-N1 for 24 h were analyzed by RT-PCR with a primer set of F13 and Rvec (B) for splicing skipping of the EP300 exon 14 (F). Percentage of the EP300 exon 14 skipping are calculated as described (B) and shown in bar graph (G) are means ± SD from two separate experiments. $^{*}P < 0.05$ and $^{**}P < 0.01$ by Student's t-test.

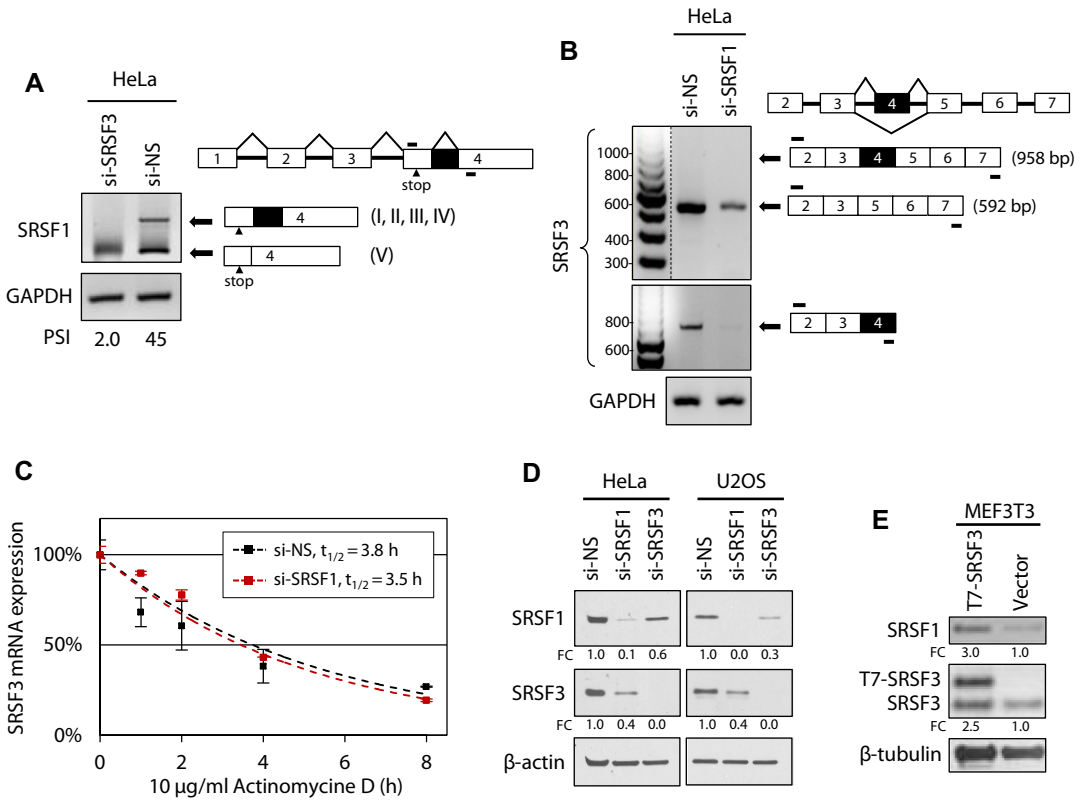

Figure 7. SRSF3 and SRSF1 are mutually regulated in cells. (**A**) SRSF3 knockdown in HeLa cells activates the usage of a cryptic intron in the SRSF1 exon 4. HeLa cells were transfected with Dharmacon si-NS or si-SRSF3 as described in Figure 4 and total RNA from the cells was analyzed by RT-PCR for activation of a cryptic intron (dark box) in the SRSF1 3′ UTR. (**B**) Knocking down SRSF1 expression in HeLa cells affects SRSF3 transcript level, but not inclusion or skipping of the SRSF3 exon 4. Knockdown of SRSF1 expression in HeLa cells was performed as described in Figure 4. See other details in Figure 3. (**C**) Knocking down SRSF1 expression in HeLa cells does not affect SRSF3 RNA stability in a pause-chase RNA decay assay. Following 10 μg/ml actinomycin D treatment for 0, 1, 2, 4 and 8 h, HeLa cells with Dharmacon si-NS or si-SRSF1 knockdown as described in Figure 4 were examined for the quantitative levels of the exon 4-skipped SRSF3 RNA and GAPDH RNA at each time point by quantitative RT-qPCR. After normalizing to GAPDH RNA, the exon 4-skipped SRSF3 RNA decay rate was calculated by setting the RNA levels at 0 h as 100% for both si-NS and si-SRSF1 groups. Exponential fitting curves over each time point are determined as $y = e^{-0.185x}$, $R^2 = 0.8739$ for si-NS group and $y = e^{-0.201x}$, $R^2 = 0.9819$ for si-SRSF1 group. Half-life ($t_{1/2}$) of the exon 4-skipped SRSF3 RNA was calculated as 3.8 h for si-NS transfected cells, and 3.5 h for si-SRSF1 transfected cells. (**D**) Expression of SRSF3 and SRSF1 is mutually regulated each other. HeLa or U2OS cells were transfected with Dharmacon si-NS, si-SRSF1, or si-SRSF3 twice with an interval of 48 h, and analyzed by Western blot for the corresponding protein expression by using an anti-SRSF1 or anti-SRSF3 antibody. (**E**) Overexpression of T7-SRSF3 increases the expression of SRSF1 in MEF3T3 cells revealed by Western blot.

ditional three nucleotide mutations outside of the mutant motif c (Figure 6D) and binding both PTB and ∼30-kDa SR protein (Figure 6E) showed much more skipping of the exon 14 than the mt-1 (Figure 6F and G). Altogether, our data conclude that the binding of SRSF3 to this region is necessary for inclusion of the exon 14 in EP300 mRNA.

SRSF3 and SRSF1 are mutually regulated in cells and both display increased expression in cancer cells

Given SRSF3 regulates the alternative splicing of SRSF1 RNA (Figure 7A), we next examined whether knockdown of SRSF1 expression could also affect alternative splicing of SRSF3 pre-mRNA which contains seven exons, with the exon 4-skipped mRNA to encode full-length SRSF3 and the exon 4-included mRNA to produce a truncated SRSF3 lacking the RS domain (66). We found that knockdown of SRSF1 expression in HeLa cells does not promote inclusion of the exon 4 during SRSF3 RNA splicing, but rather affects SRSF3 transcription (Figure 7B). This was independent of the RNA degradation, because knockdown of SRSF1 expression in HeLa cells did not affect the decay rate of the exon 4-skipped SRSF3 RNA (Figure 7C). Consistent with these observations, Western blotting analysis showed that knocking down SRSF1 expression in HeLa or U2OS cells reduces the production of SRSF3 proteins. Conversely, knocking down SRSF3 in these two types of cells also reduces the protein level of the SRSF1 (isoform 1) (Figure 7D). Moreover, overexpression of SRSF3 in mouse embryo fibroblast MEF3T3 cells increases the level of endogenous SRSF1 protein (Figure 7E). These data clearly indicate that SRSF3 and SRSF1 are mutually regulated during their expression. The notion was further supported by their coexpression in normal cervical tissues using immunohistochemistry staining (Supplementary Figure S5) and by Western blot analysis in comparing human fetal normal lung fibroblast MRC-5 (diploid male) and WI-38 (diploid female) cells with cancer-derived cell lines U2OS and HeLa cells (Figure 8A). We showed that both SRSF1 and SRSF3 proteins in normal cervix exhibit a similar basal and parabasal

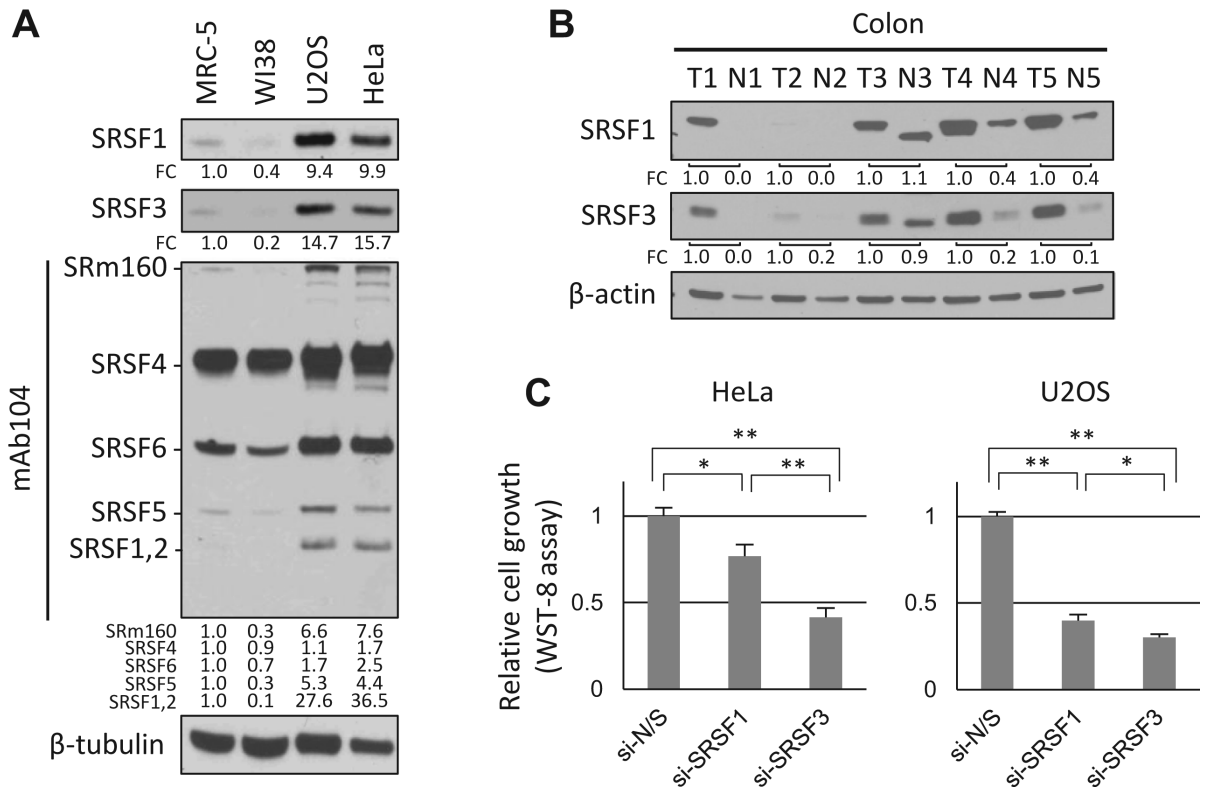

Figure 8. SRSF3 and SRSF1 are mutually regulated in cell lines and coexpressed in normal and cancer cells. (**A**) SRSF3 and SRSF1 are coexpressed along with SRm160, SRSF5, SRSF2 and SRSF9, but only moderately with SRSF4 and SRSF6 in MRC-5, WI-38, U2OS and HeLa cells. Cell lysates for blotting SRSF3 in our previous publication (28) were reprobed by anti-SRSF1 or a pan-SR protein antibody mAb104. (**B**) Several paired (tumor versus tumor-adjacent normal tissues) samples from colon cancers were compared by Western blot assays for SRSF1 and SRSF3 coexpression. β-actin or β-tubulin served as a loading control for individual Western blot assay. FC, fold-change. (**C**) WST-8 assay for cell proliferation of HeLa and U2OS cells. Mean ± SD were calculated from three biological repeats. $*P < 0.05$ and $**P < 0.01$ by Student's *t*-test.

nuclear expression profile to SRSF2, hnRNP K, hnRNP L, hnRNP A1 and YB-1, which show more basal than parabasal nuclear expression, but different from involucrin and ANXA1, two cytoplasmic proteins expressing very little in the proliferating basal cells (Supplementary Figure S5). Both SRSF1 and SRSF3 exhibit a similar expression profile, with more proteins in U2OS and HeLa cells than that in MRC-5 and WI-38 cells, as seen for SRm160, SRSF5 and SRSF2, whereas SRSF4 and SRSF6 exhibit a similar amount of protein expression among all four cell types (Figure 8A). Since SRSF1 in overexpression functions as a proto-oncogene in cells (67–69) as SRSF3 does (28), their mutual regulation would be synergic and crucial for their oncogenic potentials. We observed that both SRSF1 and SRSF3 display a remarkable increase in colon cancer tissues (Figure 8B) and other cancer tissues of lung, breast, stomach, skin, bladder, liver and cervix as well as in lymphoma cells (Supplementary Figure S6). Cell proliferation assays showed that knocking down SRSF1 or SRSF3 expression in HeLa or U2OS cells prevents cell proliferation (Figure 8C).

SRSF3 regulates the expression of a subset of human miRNAs

Given the fact that pri-miRNA transcripts are predominantly RNA polymerase II transcripts (70) composed of exons and introns, recent studies indicate that many miRNAs produced from introns (71–73) are spliceosome subunit-dependent (73) and sensitive to a lariat debranching enzyme (74) and SRSF3 also regulates pri-miRNA processing by modulating Drosha-mediated pri-miRNA cleavage activity (19) in addition to its roles in post-transcriptional RNA processing. We further examined whether SRSF3 regulates cellular miRNA expression in addition to those coding genes discovered by our splice array assay. Total RNA isolated from HeLa cells with or without SRSF3 knockdown was analyzed by a miRNA array assay for a genome-wide expression of 856 human mature miRNAs. We found that knocking down SRSF3 in HeLa cells decreases the expression of miR-16, miR-18a, miR-21, miR-92b, miR-128, miR-182, miR-629, miR-629*, miR-1180 and miR-1308, and increases the expression of miR-7, miR-26a, miR-30a, miR-99a, miR100, miR-125b, miR-181a, miR-206, miR-378 and miR-923 (Supplementary Figure S7A and Table S7). Consistently, other studies indicate that miR-21 in miRCancer database (http://mircancer.ecu.edu) is highly expressed almost in all examined human cancers (Supplementary Table S8). Overexpression of miR-21 also causes the development of pre-B malignancy (75), but miR-21-null mice show reduction of papilloma (76). We further confirmed by Northern blotting the decreased expression of miR-21 and increased expression of miR-125b in the cells

due to SRSF3 knockdown (Supplementary Figure S7B). By TaqMan miRNA real-time quantitative PCR assays, we verified the SRSF3-targeted changes of randomly selected seven additional miRNAs, including miR-16, miR-18a, miR-128 and miR-182, of which all showed a decreased expression (Supplementary Figure S7C), and miR181a, miR-100 and miR-30a, of which all showed an increased expression, by SRSF3 knockdown (Supplementary Figure S7D).

DISCUSSION

SRSF3 is a general splicing factor and has multifunctional activities from affecting genome stability to transcription, RNA processing and protein translation (25). We and others reported that cancer tissues exhibit the increased expression of SRSF3 which is important for cancer cell proliferation and survival. Increased SRSF3 expression promotes cell immortalization and transformation and is required for tumor induction and maintenance in nude mice (28,32). To date, only a few endogenous RNA targets of SRSF3 in human cells have been reported (16,28,35–38,66,77). In this study, we compiled a global atlas of SRSF3-regulated differential gene expression and splicing events by knocking down SRSF3 expression in human cells. We uncovered more than 200 of SRSF3-targets that are related to cell growth and cycle, cytoskeleton, and RNA splicing. Global analysis of SRSF3-specific mRNPs by ectopic expression of GFP-tagged SRSF3 in mouse neural p19 cells has revealed hundreds of transcripts that change in response to neural differentiation and cell cycles (41). However, the two different approaches conducted in different cell types from different species exhibit largely non-overlapping SRSF3 targets.

Among the validated transcription and splicing event from the SRSF3-targeted genes identified by the B/E ratio method or the ANOVA assay, ERRFI1 and ANXA1 are two tumor suppressors (78,79) and TGFβ2 promotes metastasis in multiple types of cancer (80–82). Knocking down SRSF3 expression increases the expression of ERRFI1 and ANXA1, but decreases the expression of TGFβ2. Although SRSF3 knockdown induces the selection of an alternative 5′ ss in the exon 3 of PUS3 (83) and an alternative 3′ ss in the exon 3 of Sp1 (10,84–86) as well as activation of a cryptic intron in the 3′-UTR of SRSF1 (69,87), the most affected events from SRSF3 knockdown are induction of exon skipping, leading to aberrant gene expression. Further analyses indicate that skipping of the exon 7 in PKP4 (88,89) creates a premature stop codon, exon 18 in KIF23 (90) produces a short isoform of KIF23, exon 14 in EP300 (63–65) produces a truncated protein p300ΔE14, exon 11 in CLINT1 (91) creates a premature stop codon, exon 3 in CHK1(92) creates a premature stop codon, exons 3–4 in SMC2 (93) induces in-frame deletion of 91 residues in the N-terminal region, exon 3 in CKLF(94,95) induces in-frame deletion of 53 residues, exon 10 in MAP4 (96) deletes 72 residues in the Pro-rich region (97), exon 4 in MBNL1 (98,99) causes an in-frame deletion of 68 residues (100), exon 11 in MELK (101,102) induces an in-frame deletion of 29 residues, exon 12 in DDX5(103,104) deletes 75 residues and exons 10–11 in PABPC1(50,105–107) causes a frameshift to produce a smaller protein missing the C-terminal MLLE domain (108,109).

A few of SRSF3 targets previously reported are not on our top list, but in the submitted NCBI GEO Datasets (accession number GSE22149). For instance, the splice array showed increased inclusion of FoxM1 exon 9 following SRSF3 knockdown (2.04-fold-change, $P = 0.0493$), which is consistent with the finding that SRSF3 promotes exon 9 skipping of FoxM1 (28). Similarly, SRSF3 regulates PKM2 (pyruvate kinase M2) exon 10 inclusion (36). We found that SRSF3 knockdown increases skipping of PKM2 exon 10 (1.23-fold-change, $P = 0.0071$). Together with a successful validation rate of ∼91% (Supplementary Table S5) for those SRSF3-targeted transcripts on the B/E top list and of ∼82% (Supplementary Table S5) for those SRSF3 targets on the ANOVA top list by RT-PCR, our study certainly provides a reliable and large splice array dataset for future studies.

Although our splice array approach using human U2OS cells with SRSF3 knockdown was very different from a CLIP approach using mouse neural p19 cells with ectopic overexpression of GFP-SRSF3 (42), we do have some common interesting observations. First, the enriched SFSF3-binding motifs, CCAG(C/G)C and (A/G)CAGCA, from the regulated splicing events in our study are very similar to the identified SRSF3-binding motifs (C/U)(A/C/U)(U/A)(C/A/U)(A/C/U) by a CLIP assay (42). Second, the enriched motifs in our study are found frequently ∼50–150 nts from a splice site in the regulated exons. Consistently, other study also showed that the most pronounced SRSF3 binding sites are seen mostly in the exon within 100 nts from the splice site although they could be a few hundred nucleotides upstream or downstream of a splice site (42). More importantly, the identified motif 1 and motif 2 bind SRSF3 and regulates skipping/inclusion of an alternative exon. Disruption of a SRSF3-binding site in the EP300 exon 14 by deletion or introduction of point mutations was found to induce exon 14 skipping and produce a truncated protein p300ΔE14.

SRSF3 regulates the expression of other members of the SR protein family (42) and modulates its own expression (66). Although SRSF1, when ectopically expressed, was found to inhibit exon 4 inclusion of SRSF3 from an expression vector (110), how endogenous SRSF1 affects SRSF3 expression remains unknown. In this report, we provide further evidence that endogenous SRSF1 and SRSF3 are mutually regulated and co-expressed in normal and cancer cells/tissues. In addition, SRSF1, 2, 3, 5 and SRm160 are also upregulated in cancer cell lines U2OS and HeLa, but not in the immortalized, non-transformed MRC-5 and WI38 fibroblast lines. On the other hand, SRSF4 and SRSF6 show little difference in their expression in all four cell lines examined. Data indicate the SRSF4 and SRSF6 might be less sensitive to mutual regulation by other SR proteins. Similar to SRSF3, SRSF1 is another oncogenic splicing factor in association with various types of cancer (67–69). Both SRSF1 and SRSF3 mediate several overlapping oncogenic phenotypes, such as anti-apoptosis, anchorage-independent cell growth and tumor formation in nude mice (28,37,68,69,111). However, SRSF3 prevents activation of

cryptic intron splicing in the SRSF1 exon 4, whereas SRSF1 preferentially affect SRSF3 transcription.

In addition to its post-transcriptional roles in regulation of various coding or non-coding pol II gene expression, SRSF3 modulates pri-miRNA processing by Drosha via binding to a CNNC motif downstream of most pri-miRNA hairpins in animals (19). We found that SRSF3 regulates the expression of a subset of miRNAs. It remains to be determined whether SRSF3 regulates these identified miRNAs through the proposed pathway (19) or by modulating RNA splicing (73,74). However, our finding on SRSF3 regulation of miR-16 production is consistent with the report that SRSF3 enhances miR-16 processing in a CNNC-dependent manner (19). By searching the miRCancer database (http://mircancer.ecu.edu) for all SRSF3-regulated miRNAs identified in this study, we found that the miR18a, miR-21, miR-92b and miR-182, which are oncomiRs, and the miR-7, miR-26a, miR-30, miR-99a, miR-100 and miR-206, which are tumor-suppressive miRNAs, display a close correlation in the expression to SRSF3. In searching the miRTarBase database (http://mirtarbase.mbc.nctu.edu.tw/) for miR-21 targets, we found that the four miR-21 target genes (EDIL3, PER3, TGFB2 and TNFAIP3) are also the SRSF3 targets for the gene expression changes (Figure 1C). Together we provide multiple lines of evidence indicating that SRSF3's oncogenic activity might be mediated through a complex network of those targeted genes and miRNAs.

SUPPLEMENTARY DATA

Supplementary Data are available at NAR Online.

ACKNOWLEDGEMENT

We thank Kang Tu for his initial work on ANOVA analysis.

FUNDING

Intramural Research Program of National Cancer Institute and National Heart, Lung, and Blood Institute; National Institutes of Health. Funding for open access charge: Intramural Research Program of National Cancer Institute, National Institutes of Health.
Conflict of interest statement. None declared.

REFERENCES

1. Wang,E.T., Sandberg,R., Luo,S., Khrebtukova,I., Zhang,L., Mayr,C., Kingsmore,S.F., Schroth,G.P. and Burge,C.B. (2008) Alternative isoform regulation in human tissue transcriptomes. *Nature*, **456**, 470–476.
2. Charizanis,K., Lee,K.Y., Batra,R., Goodwin,M., Zhang,C., Yuan,Y., Shiue,L., Cline,M., Scotti,M.M., Xia,G. *et al.* (2012) Muscleblind-like 2-mediated alternative splicing in the developing brain and dysregulation in myotonic dystrophy. *Neuron*, **75**, 437–450.
3. Weyn-Vanhentenryck,S.M., Mele,A., Yan,Q., Sun,S., Farny,N., Zhang,Z., Xue,C., Herre,M., Silver,P.A., Zhang,M.Q. *et al.* (2014) HITS-CLIP and integrative modeling define the Rbfox splicing-regulatory network linked to brain development and autism. *Cell Rep.*, **6**, 1139–1152.
4. Burghes,A.H. and Beattie,C.E. (2009) Spinal muscular atrophy: why do low levels of survival motor neuron protein make motor neurons sick? *Nat. Rev. Neurosci.*, **10**, 597–609.
5. Pittman,A.M., Fung,H.C. and de,S.R. (2006) Untangling the tau gene association with neurodegenerative disorders. *Hum. Mol. Genet.*, **15**, R188–R195.
6. Zhang,J. and Manley,J.L. (2013) Misregulation of pre-mRNA alternative splicing in cancer. *Cancer Discov.*, **3**, 1228–1237.
7. Xiong,H.Y., Alipanahi,B., Lee,L.J., Bretschneider,H., Merico,D., Yuen,R.K., Hua,Y., Gueroussov,S., Najafabadi,H.S., Hughes,T.R. *et al.* (2015) RNA splicing. The human splicing code reveals new insights into the genetic determinants of disease. *Science*, **347**, 1254806.
8. Zahler,A.M., Lane,W.S., Stolk,J.A. and Roth,M.B. (1992) SR proteins: a conserved family of pre-mRNA splicing factors. *Genes Dev.*, **6**, 837–847.
9. Manley,J.L. and Krainer,A.R. (2010) A rational nomenclature for serine/arginine-rich protein splicing factors (SR proteins). *Genes Dev.*, **24**, 1073–1074.
10. Jia,R., Liu,X., Tao,M., Kruhlak,M., Guo,M., Meyers,C., Baker,C.C. and Zheng,Z.M. (2009) Control of the papillomavirus early-to-late switch by differentially expressed SRp20. *J. Virol.*, **83**, 167–180.
11. Majerciak,V., Lu,M., Li,X. and Zheng,Z.M. (2014) Attenuation of the suppressive activity of cellular splicing factor SRSF3 by Kaposi sarcoma-associated herpesvirus ORF57 protein is required for RNA splicing. *RNA.*, **20**, 1747–1758.
12. Huang,Y. and Steitz,J.A. (2001) Splicing factors SRp20 and 9G8 promote the nucleocytoplasmic export of mRNA. *Mol. Cell*, **7**, 899–905.
13. Escudero-Paunetto,L., Li,L., Hernandez,F.P. and Sandri-Goldin,R.M. (2010) SR proteins SRp20 and 9G8 contribute to efficient export of herpes simplex virus 1 mRNAs. *Virology*, **401**, 155–164.
14. Lou,H., Neugebauer,K.M., Gagel,R.F. and Berget,S.M. (1998) Regulation of alternative polyadenylation by U1 snRNPs and SRp20. *Mol. Cell Biol.*, **18**, 4977–4985.
15. Maciolek,N.L. and McNally,M.T. (2007) Serine/arginine-rich proteins contribute to negative regulator of splicing element-stimulated polyadenylation in rous sarcoma virus. *J. Virol.*, **81**, 11208–11217.
16. Kim,J., Park,R.Y., Chen,J.K., Kim,J., Jeong,S. and Ohn,T. (2014) Splicing factor SRSF3 represses the translation of programmed cell death 4 mRNA by associating with the 5′-UTR region. *Cell Death. Differ.*, **21**, 481–490.
17. Fitzgerald,K.D. and Semler,B.L. (2011) Re-localization of cellular protein SRp20 during poliovirus infection: bridging a viral IRES to the host cell translation apparatus. *PLoS Pathog.*, **7**, e1002127.
18. Bedard,K.M., Daijogo,S. and Semler,B.L. (2007) A nucleo-cytoplasmic SR protein functions in viral IRES-mediated translation initiation. *EMBO J.*, **26**, 459–467.
19. Auyeung,V.C., Ulitsky,I., McGeary,S.E. and Bartel,D.P. (2013) Beyond secondary structure: primary-sequence determinants license pri-miRNA hairpins for processing. *Cell*, **152**, 844–858.
20. Loomis,R.J., Naoe,Y., Parker,J.B., Savic,V., Bozovsky,M.R., Macfarlan,T., Manley,J.L. and Chakravarti,D. (2009) Chromatin binding of SRp20 and ASF/SF2 and dissociation from mitotic chromosomes is modulated by histone H3 serine 10 phosphorylation. *Mol. Cell*, **33**, 450–461.
21. Bavelloni,A., Faenza,I., Cioffi,G., Piazzi,M., Parisi,D., Matic,I., Maraldi,N.M. and Cocco,L. (2006) Proteomic-based analysis of nuclear signaling: PLCbeta1 affects the expression of the splicing factor SRp20 in Friend erythroleukemia cells. *Proteomics.*, **6**, 5725–5734.
22. Sen,S., Talukdar,I. and Webster,N.J. (2009) SRp20 and CUG-BP1 modulate insulin receptor exon 11 alternative splicing. *Mol. Cell. Biol.*, **29**, 871–880.
23. Saeki,K., Yasugi,E., Okuma,E., Breit,S.N., Nakamura,M., Toda,T., Kaburagi,Y. and Yuo,A. (2005) Proteomic analysis on insulin signaling in human hematopoietic cells: identification of CLIC1 and SRp20 as novel downstream effectors of insulin. *Am. J. Physiol. Endocrinol. Metab.*, **289**, E419–E428.
24. Corbo,C., Orru,S., Gemei,M., Noto,R.D., Mirabelli,P., Imperlini,E., Ruoppolo,M., Vecchio,L.D. and Salvatore,F. (2012) Protein cross-talk in CD133+ colon cancer cells indicates activation of the Wnt pathway and upregulation of SRp20 that is potentially involved in tumorigenicity. *Proteomics.*, **12**, 2045–2059.

25. Corbo,C., Orru,S. and Salvatore,F. (2013) SRp20: an overview of its role in human diseases. *Biochem. Biophys. Res. Commun.*, **436**, 1–5.
26. Chen,W., Itoyama,T. and Chaganti,R.S. (2001) Splicing factor SRP20 is a novel partner of BCL6 in a t(3;6)(q27;p21) translocation in transformed follicular lymphoma. *Genes Chromosomes Cancer*, **32**, 281–284.
27. Watanuki,T., Funato,H., Uchida,S., Matsubara,T., Kobayashi,A., Wakabayashi,Y., Otsuki,K., Nishida,A. and Watanabe,Y. (2008) Increased expression of splicing factor SRp20 mRNA in bipolar disorder patients. *J. Affect. Disord.*, **110**, 62–69.
28. Jia,R., Li,C., McCoy,J.P., Deng,C.X. and Zheng,Z.M. (2010) SRp20 is a proto-oncogene critical for cell proliferation and tumor induction and maintenance. *Int. J. Biol. Sci.*, **6**, 806–826.
29. Wong,J., Garner,B., Halliday,G.M. and Kwok,J.B. (2012) Srp20 regulates TrkB pre-mRNA splicing to generate TrkB-Shc transcripts with implications for Alzheimer's disease. *J. Neurochem.*, **123**, 159–171.
30. Sen,S., Langiewicz,M., Jumaa,H. and Webster,N.J. (2015) Deletion of serine/arginine-rich splicing factor 3 in hepatocytes predisposes to hepatocellular carcinoma in mice. *Hepatology*, **61**, 171–183.
31. He,X., Ee,P.L., Coon,J.S. and Beck,W.T. (2004) Alternative splicing of the multidrug resistance protein 1/ATP binding cassette transporter subfamily gene in ovarian cancer creates functional splice variants and is associated with increased expression of the splicing factors PTB and SRp20. *Clin. Cancer Res.*, **10**, 4652–4660.
32. He,X., Arslan,A.D., Pool,M.D., Ho,T.T., Darcy,K.M., Coon,J.S. and Beck,W.T. (2011) Knockdown of splicing factor SRp20 causes apoptosis in ovarian cancer cells and its expression is associated with malignancy of epithelial ovarian cancer. *Oncogene*, **30**, 356–365.
33. Iborra,S., Hirschfeld,M., Jaeger,M., Zur,H.A., Braicu,I., Sehouli,J., Gitsch,G. and Stickeler,E. (2013) Alterations in expression pattern of splicing factors in epithelial ovarian cancer and its clinical impact. *Int. J. Gynecol. Cancer*, **23**, 990–996.
34. Kurokawa,K., Akaike,Y., Masuda,K., Kuwano,Y., Nishida,K., Yamagishi,N., Kajita,K., Tanahashi,T. and Rokutan,K. (2014) Downregulation of serine/arginine-rich splicing factor 3 induces G1 cell cycle arrest and apoptosis in colon cancer cells. *Oncogene*, **33**, 1407–1417.
35. Jang,H.N., Lee,M., Loh,T.J., Choi,S.W., Oh,H.K., Moon,H., Cho,S., Hong,S.E., Kim,d.H., Sheng,Z. *et al.* (2014) Exon 9 skipping of apoptotic caspase-2 pre-mRNA is promoted by SRSF3 through interaction with exon 8. *Biochim. Biophys. Acta*, **1839**, 25–32.
36. Wang,Z., Chatterjee,D., Jeon,H.Y., Akerman,M., Vander Heiden,M.G., Cantley,L.C. and Krainer,A.R. (2012) Exon-centric regulation of pyruvate kinase M alternative splicing via mutually exclusive exons. *J. Mol. Cell Biol.*, **4**, 79–87.
37. Tang,Y., Horikawa,I., Ajiro,M., Robles,A.I., Fujita,K., Mondal,A.M., Stauffer,J.K., Zheng,Z.M. and Harris,C.C. (2013) Downregulation of splicing factor SRSF3 induces p53beta, an alternatively spliced isoform of p53 that promotes cellular senescence. *Oncogene*, **32**, 2792–2798.
38. Walsh,C.M., Suchanek,A.L., Cyphert,T.J., Kohan,A.B., Szeszel-Fedorowicz,W. and Salati,L.M. (2013) Serine arginine splicing factor 3 is involved in enhanced splicing of glucose-6-phosphate dehydrogenase RNA in response to nutrients and hormones in liver. *J. Biol. Chem.*, **288**, 2816–2828.
39. Sen,S., Jumaa,H. and Webster,N.J. (2013) Splicing factor SRSF3 is crucial for hepatocyte differentiation and metabolic function. *Nat. Commun.*, **4**, 1336.
40. Ohta,S., Nishida,E., Yamanaka,S. and Yamamoto,T. (2013) Global splicing pattern reversion during somatic cell reprogramming. *Cell Rep.*, **5**, 357–366.
41. Anko,M.L., Morales,L., Henry,I., Beyer,A. and Neugebauer,K.M. (2010) Global analysis reveals SRp20- and SRp75-specific mRNPs in cycling and neural cells. *Nat. Struct. Mol. Biol.*, **17**, 962–970.
42. Anko,M.L., Muller-McNicoll,M., Brandl,H., Curk,T., Gorup,C., Henry,I., Ule,J. and Neugebauer,K.M. (2012) The RNA-binding landscapes of two SR proteins reveal unique functions and binding to diverse RNA classes. *Genome Biol.*, **13**, R17.
43. Tao,M., Kruhlak,M., Xia,S., Androphy,E. and Zheng,Z.M. (2003) Signals that dictate nuclear localization of human papillomavirus type 16 oncoprotein E6 in living cells. *J. Virol.*, **77**, 13232–13247.
44. Zheng,Z.M., Reid,E.S. and Baker,C.C. (2000) Utilization of the bovine papillomavirus type 1 late-stage-specific nucleotide 3605 3′ splice site is modulated by a novel exonic bipartite regulator but not by an intronic purine-rich element. *J. Virol.*, **74**, 10612–10622.
45. Solier,S., Barb,J., Zeeberg,B.R., Varma,S., Ryan,M.C., Kohn,K.W., Weinstein,J.N., Munson,P.J. and Pommier,Y. (2010) Genome-wide analysis of novel splice variants induced by topoisomerase I poisoning shows preferential occurrence in genes encoding splicing factors. *Cancer Res.*, **70**, 8055–8065.
46. Smyth,G.K., Michaud,J. and Scott,H.S. (2005) Use of within-array replicate spots for assessing differential expression in microarray experiments. *Bioinformatics.*, **21**, 2067–2075.
47. Benjamini,Y., Drai,D., Elmer,G., Kafkafi,N. and Golani,I. (2001) Controlling the false discovery rate in behavior genetics research. *Behav. Brain Res.*, **125**, 279–284.
48. Bailey,T.L., Williams,N., Misleh,C. and Li,W.W. (2006) MEME: discovering and analyzing DNA and protein sequence motifs. *Nucleic Acids Res.*, **34**, W369–W373 .
49. Bailey,T.L., Boden,M., Buske,F.A., Frith,M., Grant,C.E., Clementi,L., Ren,J., Li,W.W. and Noble,W.S. (2009) MEME SUITE: tools for motif discovery and searching. *Nucleic Acids Res.*, **37**, W202–W208.
50. Massimelli,M.J., Kang,J.G., Majerciak,V., Le,S.Y., Liewehr,D.J., Steinberg,S.M. and Zheng,Z.M. (2011) Stability of a long noncoding viral RNA depends on a 9-nt core element at the RNA 5′ end to interact with viral ORF57 and cellular PABPC1. *Int. J. Biol. Sci.*, **7**, 1145–1160.
51. Majerciak,V., Uranishi,H., Kruhlak,M., Pilkington,G.R., Massimelli,M.J., Bear,J., Pavlakis,G.N., Felber,B.K. and Zheng,Z.M. (2011) Kaposi's sarcoma-associated herpesvirus ORF57 interacts with cellular RNA export cofactors RBM15 and OTT3 to promote expression of viral ORF59. *J. Virol.*, **85**, 1528–1540.
52. Livak,K.J. and Schmittgen,T.D. (2001) Analysis of relative gene expression data using real-time quantitative PCR and the 2(-Delta Delta C(T)) Method. *Methods*, **25**, 402–408.
53. Ajiro,M., Katagiri,T., Ueda,K., Nakagawa,H., Fukukawa,C., Lin,M.L., Park,J.H., Nishidate,T., Daigo,Y. and Nakamura,Y. (2009) Involvement of RQCD1 overexpression, a novel cancer-testis antigen, in the Akt pathway in breast cancer cells. *Int. J. Oncol.*, **35**, 673–681.
54. Ajiro,M. and Zheng,Z.M. (2015) E6^E7, a novel splice isoform protein of human papillomavirus 16, stabilizes viral E6 and E7 oncoproteins via HSP90 and GRP78. *MBio.*, **6**, doi:10.1128/mBio.02068-14.
55. Ueki,T., Park,J.H., Nishidate,T., Kijima,K., Hirata,K., Nakamura,Y. and Katagiri,T. (2009) Ubiquitination and downregulation of BRCA1 by ubiquitin-conjugating enzyme E2T overexpression in human breast cancer cells. *Cancer Res.*, **69**, 8752–8760.
56. Cheng,A.W., Shi,J., Wong,P., Luo,K.L., Trepman,P., Wang,E.T., Choi,H., Burge,C.B. and Lodish,H.F. (2014) Muscleblind-like 1 (Mbnl1) regulates pre-mRNA alternative splicing during terminal erythropoiesis. *Blood*, **124**, 598–610.
57. Schneider,C.A., Rasband,W.S. and Eliceiri,K.W. (2012) NIH Image to ImageJ: 25 years of image analysis. *Nat. Methods*, **9**, 671–675.
58. Falcon,S. and Gentleman,R. (2007) Using GOstats to test gene lists for GO term association. *Bioinformatics.*, **23**, 257–258.
59. Wang,X., Tang,S., Le,S.Y., Lu,R., Rader,J.S., Meyers,C. and Zheng,Z.M. (2008) Aberrant expression of oncogenic and tumor-suppressive microRNAs in cervical cancer is required for cancer cell growth. *PLoS One.*, **3**, e2557.
60. Wang,X., Wang,H.-K., McCoy,J.P., Banerjee,N.S., Rader,J.S., Broker,T.R., Meyers,C., Chow,L.T. and Zheng,Z.M. (2009) Oncogenic HPV infection interrupts the expression of tumor-suppressive miR-34a through viral oncoprotein E6. *RNA*, **15**, 637–647.
61. Wang,X., Wang,H.K., Li,Y., Hafner,M., Banerjee,N.S., Tang,S., Briskin,D., Meyers,C., Chow,L.T., Xie,X. *et al.* (2014) microRNAs are biomarkers of oncogenic human papillomavirus infections. *Proc. Natl. Acad. Sci. U.S.A.*, **111**, 4262–4267.
62. Stickeler,E., Fraser,S.D., Honig,A., Chen,A.L., Berget,S.M. and Cooper,T.A. (2001) The RNA binding protein YB-1 binds A/C-rich exon enhancers and stimulates splicing of the CD44 alternative exon v4. *EMBO J.*, **20**, 3821–3830.
63. Goodman,R.H. and Smolik,S. (2000) CBP/p300 in cell growth, transformation, and development. *Genes Dev.*, **14**, 1553–1577.

64. Iyer,N.G., Ozdag,H. and Caldas,C. (2004) p300/CBP and cancer. *Oncogene*, **23**, 4225–4231.
65. Ogryzko,V.V., Schiltz,R.L., Russanova,V., Howard,B.H. and Nakatani,Y. (1996) The transcriptional coactivators p300 and CBP are histone acetyltransferases. *Cell*, **87**, 953–959.
66. Jumaa,H., Guenet,J.L. and Nielsen,P.J. (1997) Regulated expression and RNA processing of transcripts from the Srp20 splicing factor gene during the cell cycle. *Mol. Cell. Biol.*, **17**, 3116–3124.
67. Das,S. and Krainer,A.R. (2014) Emerging functions of SRSF1, splicing factor and oncoprotein, in RNA metabolism and cancer. *Mol. Cancer Res.*, **12**, 1195–1204.
68. Anczukow,O., Rosenberg,A.Z., Akerman,M., Das,S., Zhan,L., Karni,R., Muthuswamy,S.K. and Krainer,A.R. (2012) The splicing factor SRSF1 regulates apoptosis and proliferation to promote mammary epithelial cell transformation. *Nat. Struct. Mol. Biol.*, **19**, 220–228.
69. Karni,R., de Stanchina,E., Lowe,S.W., Sinha,R., Mu,D. and Krainer,A.R. (2007) The gene encoding the splicing factor SF2/ASF is a proto-oncogene. *Nat. Struct. Mol. Biol.*, **14**, 185–193.
70. Lee,Y., Kim,M., Han,J., Yeom,K.H., Lee,S., Baek,S.H. and Kim,V.N. (2004) MicroRNA genes are transcribed by RNA polymerase II. *EMBO J.*, **23**, 4051–4060.
71. Berezikov,E., Chung,W.J., Willis,J., Cuppen,E. and Lai,E.C. (2007) Mammalian mirtron genes. *Mol. Cell*, **28**, 328–336.
72. Ladewig,E., Okamura,K., Flynt,A.S., Westholm,J.O. and Lai,E.C. (2012) Discovery of hundreds of mirtrons in mouse and human small RNA data. *Genome Res.*, **22**, 1634–1645.
73. Du,P., Wang,L., Sliz,P. and Gregory,R.I. (2015) A biogenesis step upstream of microprocessor controls miR-17 approximately 92 expression. *Cell*, **162**, 885–899.
74. Bortolamiol-Becet,D., Hu,F., Jee,D., Wen,J., Okamura,K., Lin,C.J., Ameres,S.L. and Lai,E.C. (2015) Selective suppression of the splicing-mediated microRNA pathway by the terminal uridyltransferase tailor. *Mol. Cell*, **59**, 217–228.
75. Medina,P.P., Nolde,M. and Slack,F.J. (2010) OncomiR addiction in an in vivo model of microRNA-21-induced pre-B-cell lymphoma. *Nature*, **467**, 86–90.
76. Ma,X., Kumar,M., Choudhury,S.N., Becker Buscaglia,L.E., Barker,J.R., Kanakamedala,K., Liu,M.F. and Li,Y. (2011) Loss of the miR-21 allele elevates the expression of its target genes and reduces tumorigenesis. *Proc. Natl. Acad. Sci. U.S.A.*, **108**, 10144–10149.
77. Galiana-Arnoux,D., Lejeune,F., Gesnel,M.C., Stevenin,J., Breathnach,R. and Gatto-Konczak,F. (2003) The CD44 alternative v9 exon contains a splicing enhancer responsive to the SR proteins 9G8, ASF/SF2, and SRp20. *J. Biol. Chem.*, **278**, 32943–32953.
78. Ferby,I., Reschke,M., Kudlacek,O., Knyazev,P., Pante,G., Amann,K., Sommergruber,W., Kraut,N., Ullrich,A., Fassler,R. *et al.* (2006) Mig6 is a negative regulator of EGF receptor-mediated skin morphogenesis and tumor formation. *Nat. Med.*, **12**, 568–573.
79. Zhang,Z., Huang,L., Zhao,W. and Rigas,B. (2010) Annexin 1 induced by anti-inflammatory drugs binds to NF-kappaB and inhibits its activation: anticancer effects in vitro and in vivo. *Cancer Res.*, **70**, 2379–2388.
80. Gordinier,M.E., Zhang,H.Z., Patenia,R., Levy,L.B., Atkinson,E.N., Nash,M.A., Katz,R.L., Platsoucas,C.D. and Freedman,R.S. (1999) Quantitative analysis of transforming growth factor beta 1 and 2 in ovarian carcinoma. *Clin. Cancer Res.*, **5**, 2498–2505.
81. Reed,J.A., McNutt,N.S. and Albino,A.P. (1994) Differential expression of basic fibroblast growth factor (bFGF) in melanocytic lesions demonstrated by in situ hybridization. Implications for tumor progression. *Am. J. Pathol.*, **144**, 329–336.
82. Friedman,E., Gold,L.I., Klimstra,D., Zeng,Z.S., Winawer,S. and Cohen,A. (1995) High levels of transforming growth factor beta 1 correlate with disease progression in human colon cancer. *Cancer Epidemiol. Biomarkers Prev.*, **4**, 549–554.
83. Chen,J. and Patton,J.R. (2000) Pseudouridine synthase 3 from mouse modifies the anticodon loop of tRNA. *Biochemistry*, **39**, 12723–12730.
84. Kaczynski,J., Cook,T. and Urrutia,R. (2003) Sp1- and Kruppel-like transcription factors. *Genome Biol.*, **4**, 206.
85. Infantino,V., Convertini,P., Iacobazzi,F., Pisano,I., Scarcia,P. and Iacobazzi,V. (2011) Identification of a novel Sp1 splice variant as a strong transcriptional activator. *Biochem. Biophys. Res. Commun.*, **412**, 86–91.
86. Apt,D., Watts,R.M., Suske,G. and Bernard,H.U. (1996) High Sp1/Sp3 ratios in epithelial cells during epithelial differentiation and cellular transformation correlate with the activation of the HPV-16 promoter. *Virology*, **224**, 281–291.
87. Sun,S., Zhang,Z., Sinha,R., Karni,R. and Krainer,A.R. (2010) SF2/ASF autoregulation involves multiple layers of post-transcriptional and translational control. *Nat. Struct. Mol. Biol.*, **17**, 306–312.
88. Keil,R., Schulz,J. and Hatzfeld,M. (2013) p0071/PKP4, a multifunctional protein coordinating cell adhesion with cytoskeletal organization. *Biol. Chem.*, **394**, 1005–1017.
89. Nahorski,M.S., Seabra,L., Straatman-Iwanowska,A., Wingenfeld,A., Reiman,A., Lu,X., Klomp,J.A., Teh,B.T., Hatzfeld,M., Gissen,P. *et al.* (2012) Folliculin interacts with p0071 (plakophilin-4) and deficiency is associated with disordered RhoA signalling, epithelial polarization and cytokinesis. *Hum. Mol. Genet.*, **21**, 5268–5279.
90. Takahashi,S., Fusaki,N., Ohta,S., Iwahori,Y., Iizuka,Y., Inagawa,K., Kawakami,Y., Yoshida,K. and Toda,M. (2012) Downregulation of KIF23 suppresses glioma proliferation. *J. Neurooncol.*, **106**, 519–529.
91. Dodd,M.E., Hatzold,J., Mathias,J.R., Walters,K.B., Bennin,D.A., Rhodes,J., Kanki,J.P., Look,A.T., Hammerschmidt,M. and Huttenlocher,A. (2009) The ENTH domain protein Clint1 is required for epidermal homeostasis in zebrafish. *Development*, **136**, 2591–2600.
92. Tse,A.N., Rendahl,K.G., Sheikh,T., Cheema,H., Aardalen,K., Embry,M., Ma,S., Moler,E.J., Ni,Z.J., Lopes de Menezes,D.E. *et al.* (2007) CHIR-124, a novel potent inhibitor of Chk1, potentiates the cytotoxicity of topoisomerase I poisons in vitro and in vivo. *Clin. Cancer Res.*, **13**, 591–602.
93. Wu,N. and Yu,H. (2012) The Smc complexes in DNA damage response. *Cell Biosci.*, **2**, 5.
94. Han,W., Lou,Y., Tang,J., Zhang,Y., Chen,Y., Li,Y., Gu,W., Huang,J., Gui,L., Tang,Y. *et al.* (2001) Molecular cloning and characterization of chemokine-like factor 1 (CKLF1), a novel human cytokine with unique structure and potential chemotactic activity. *Biochem. J.*, **357**, 127–135.
95. Yang,G.Y., Chen,X., Sun,Y.C., Ma,C.L. and Qian,G. (2013) Chemokine-like factor 1 (CLFK1) is over-expressed in patients with atopic dermatitis. *Int. J. Biol. Sci.*, **9**, 759–765.
96. Zahnleiter,D., Hauer,N.N., Kessler,K., Uebe,S., Sugano,Y., Neuhauss,S.C., Giessl,A., Ekici,A.B., Blessing,H., Sticht,H. *et al.* (2015) MAP4-dependent regulation of microtubule formation affects centrosome, cilia, and golgi architecture as a central mechanism in growth regulation. *Hum. Mutat.*, **36**, 87–97.
97. Matsushima,K., Aosaki,M., Tokuraku,K., Hasan,M.R., Nakagawa,H. and Kotani,S. (2005) Identification of a neural cell specific variant of microtubule-associated protein 4. *Cell Struct. Funct.*, **29**, 111–124.
98. Lee,J.E. and Cooper,T.A. (2009) Pathogenic mechanisms of myotonic dystrophy. *Biochem. Soc. Trans.*, **37**, 1281–1286.
99. Konieczny,P., Stepniak-Konieczna,E. and Sobczak,K. (2014) MBNL proteins and their target RNAs, interaction and splicing regulation. *Nucleic Acids Res.*, **42**, 10873–10887.
100. Kino,Y., Mori,D., Oma,Y., Takeshita,Y., Sasagawa,N. and Ishiura,S. (2004) Muscleblind protein, MBNL1/EXP, binds specifically to CHHG repeats. *Hum. Mol. Genet.*, **13**, 495–507.
101. Lin,M.L., Park,J.H., Nishidate,T., Nakamura,Y. and Katagiri,T. (2007) Involvement of maternal embryonic leucine zipper kinase (MELK) in mammary carcinogenesis through interaction with Bcl-G, a pro-apoptotic member of the Bcl-2 family. *Breast Cancer Res.*, **9**, R17.
102. Alachkar,H., Mutonga,M.B., Metzeler,K.H., Fulton,N., Malnassy,G., Herold,T., Spiekermann,K., Bohlander,S.K., Hiddemann,W., Matsuo,Y. *et al.* (2014) Preclinical efficacy of maternal embryonic leucine-zipper kinase (MELK) inhibition in acute myeloid leukemia. *Oncotarget*, **5**, 12371–12382.
103. Mazurek,A., Park,Y., Miething,C., Wilkinson,J.E., Gillis,J., Lowe,S.W., Vakoc,C.R. and Stillman,B. (2014) Acquired dependence of acute myeloid leukemia on the DEAD-box RNA helicase DDX5. *Cell Rep.*, **7**, 1887–1899.

104. Lin,S., Tian,L., Shen,H., Gu,Y., Li,J.L., Chen,Z., Sun,X., You,M.J. and Wu,L. (2013) DDX5 is a positive regulator of oncogenic NOTCH1 signaling in T cell acute lymphoblastic leukemia. *Oncogene*, **32**, 4845–4853.
105. Lemay,J.F., Lemieux,C., St-Andre,O. and Bachand,F. (2010) Crossing the borders: poly(A)-binding proteins working on both sides of the fence. *RNA Biol.*, **7**, 291–295.
106. Bag,J. and Bhattacharjee,R.B. (2010) Multiple levels of post-transcriptional control of expression of the poly (A)-binding protein. *RNA Biol.*, **7**, 5–12.
107. Massimelli,M.J., Majerciak,V., Kruhlak,M. and Zheng,Z.M. (2013) Interplay between polyadenylate-binding protein 1 and Kaposi's sarcoma-associated herpesvirus ORF57 in accumulation of polyadenylated nuclear RNA, a viral long noncoding RNA. *J. Virol.*, **87**, 243–256.
108. Kozlov,G. and Gehring,K. (2010) Molecular basis of eRF3 recognition by the MLLE domain of poly(A)-binding protein. *PLoS One.*, **5**, e10169.
109. Tritschler,F., Huntzinger,E. and Izaurralde,E. (2010) Role of GW182 proteins and PABPC1 in the miRNA pathway: a sense of deja vu. *Nat. Rev. Mol. Cell Biol.*, **11**, 379–384.
110. Jumaa,H. and Nielsen,P.J. (1997) The splicing factor SRp20 modifies splicing of its own mRNA and ASF/SF2 antagonizes this regulation. *EMBO J.*, **16**, 5077–5085.
111. Fregoso,O.I., Das,S., Akerman,M. and Krainer,A.R. (2013) Splicing-factor oncoprotein SRSF1 stabilizes p53 via RPL5 and induces cellular senescence. *Mol. Cell*, **50**, 56–66.